

Supporting Information

New inhibitors of Bcr-Abl based on 2,6,9-trisubstituted purine scaffold elicited cytotoxicity in chronic myeloid leukaemia-derived cell lines sensitive and resistant to TKIs

Thalia Delgado,¹ Denisa Veselá,² Hana Dostálová,² Vladimír Kryštof,^{2,3*} Veronika Vojáčková,² Radek Jorda,² Alejandro Castro,⁴ Jeanluc Bertrand,¹ Gildardo Ribera,⁵ Mario Faúndez,⁶ Miroslav Strnad,⁷ Christian Espinosa-Bustos⁶ and Cristian O. Salas^{1,*}

1 Departamento de Química Orgánica, Facultad de Química y de Farmacia, Pontificia Universidad Católica de Chile, Santiago de Chile 702843, Chile

2 Department of Experimental Biology, Palacký University Olomouc, Šlechtitelů 27, 783 71 Olomouc, Czech Republic

3 Institute of Molecular and Translational Medicine, Faculty of Medicine and Dentistry, Palacký University Olomouc, Hněvotínská 5, 779 00 Olomouc, Czech Republic

4 Laboratorio de Bioproductos Farmacéuticos y Cosméticos, Centro de Excelencia en Medicina Traslacional, Facultad de Medicina, Universidad de La Frontera, Av. Francisco Salazar 01145, Temuco 4780000, Chile

5 Laboratorio de Biotecnología Farmacéutica, Centro de Biotecnología Genómica, Instituto Politécnico Nacional, Boulevard del Maestro s/n, Reynosa 88710, Mexico

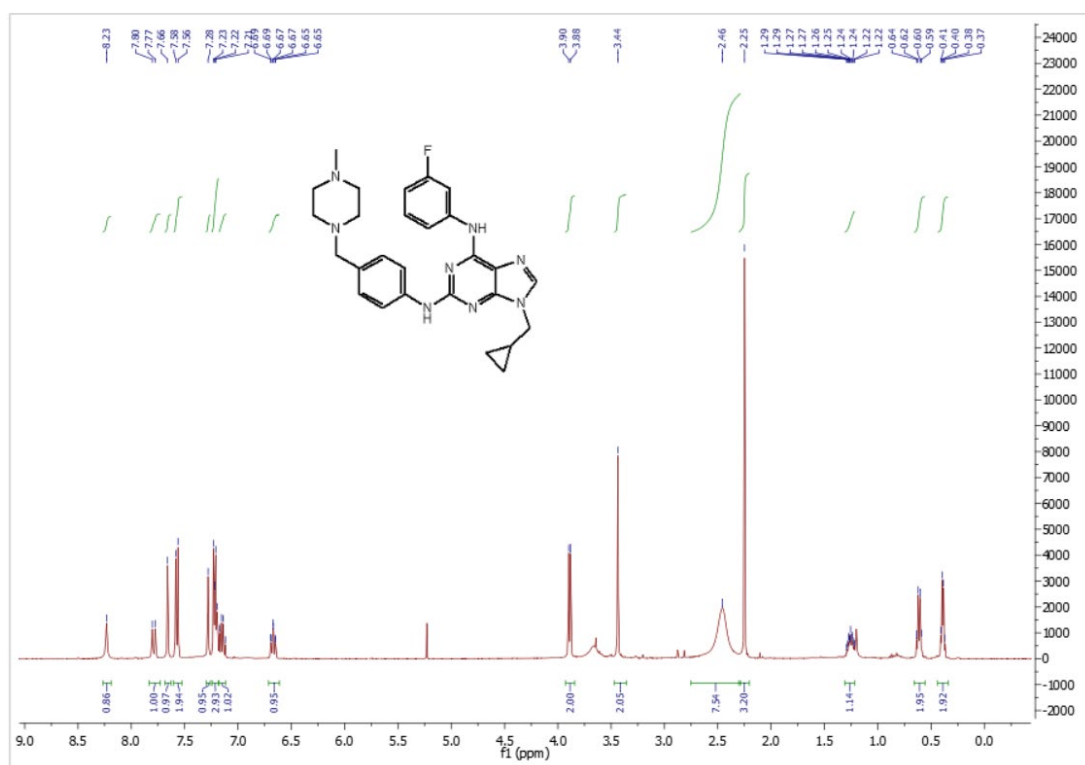
6 Departamento de Farmacia, Facultad de Química y de Farmacia, Pontificia Universidad Católica de Chile, Santiago de Chile 702843, Chile

7 Laboratory of Growth Regulators, Institute of Experimental Botany of the Czech Academy of Sciences & Palacký University, Šlechtitelů 27, 783 71 Olomouc, Czech Republic

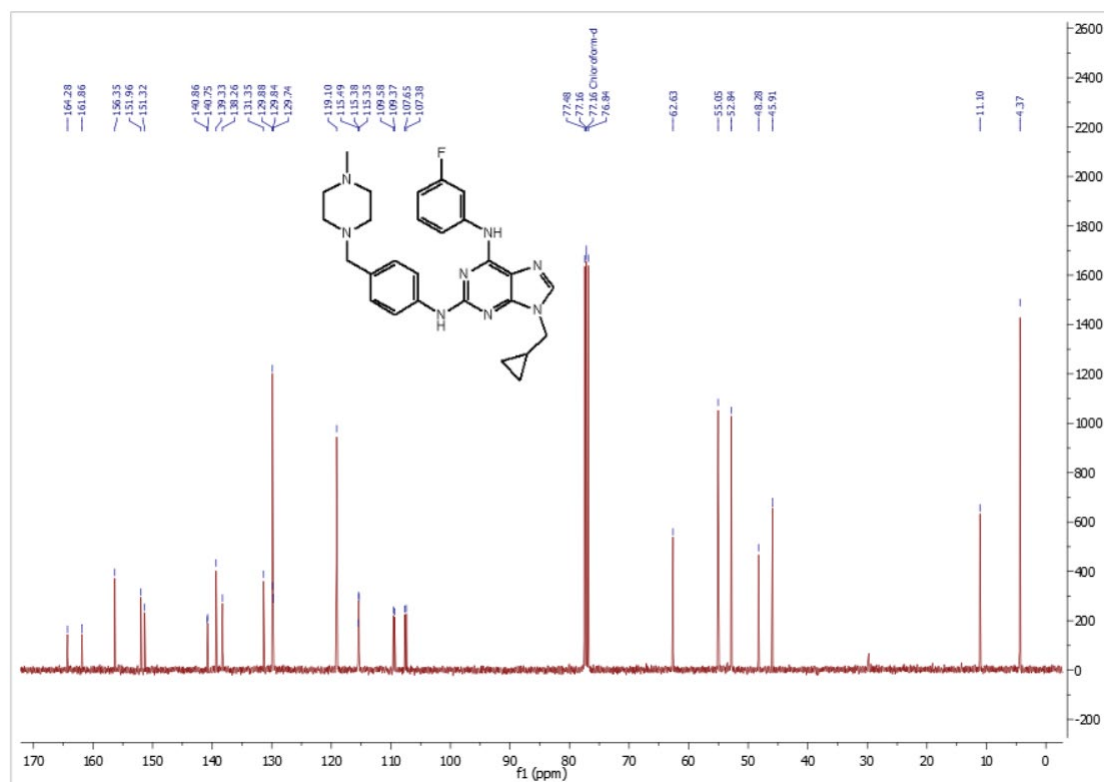
Index

¹ H, ¹³ C NMR and ¹⁹ F spectra of final compounds.....	2-19
HRMS of final compounds.....	20-26
Table S1. Binding affinity scores of the purine derivatives in the Bcr-Abl ^{WT}	pag 27
Figure S1. Co-crystallized ligand, purvalanol, in the Bcr-Abl binding site.....	pag 28
Figure S2. Correlation plot between biological activity in pIC ₅₀ and affinity energies of the synthesised compounds.....	pag 29
Figure S3. Correlation plot between biological activity in pGI ₅₀ values on B8 cells and affinity energies of the selected compounds.....	pag30
Figure S4. Histograms of flow cytometry of selected compounds on KCL cells and their subclones.....	pag31-33

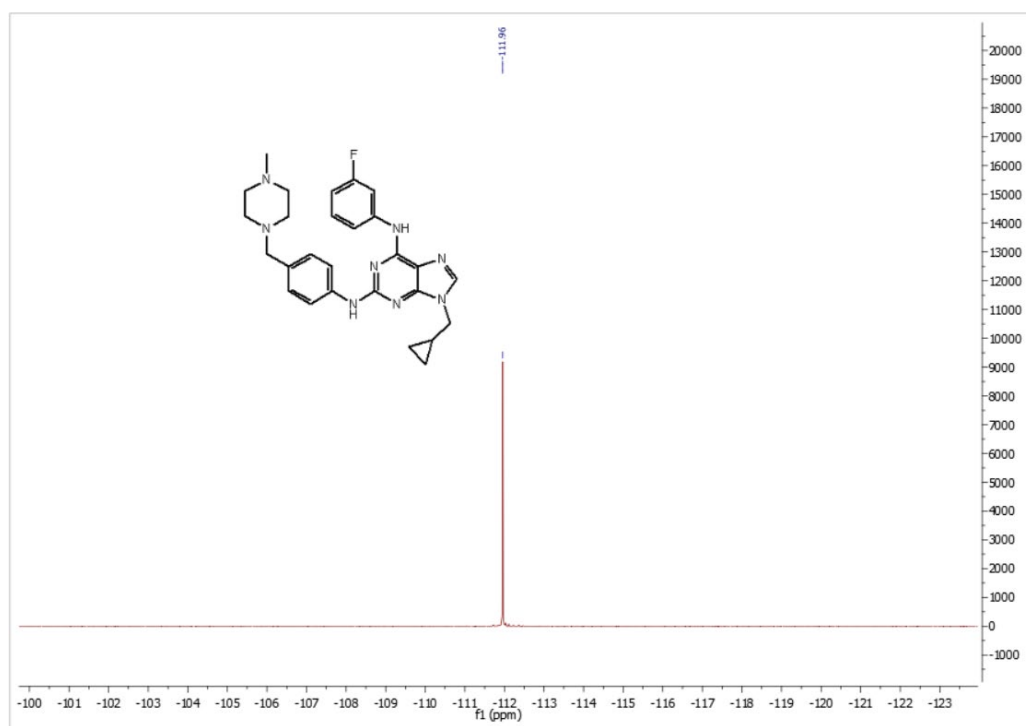
^1H NMR spectra of compound **7a**



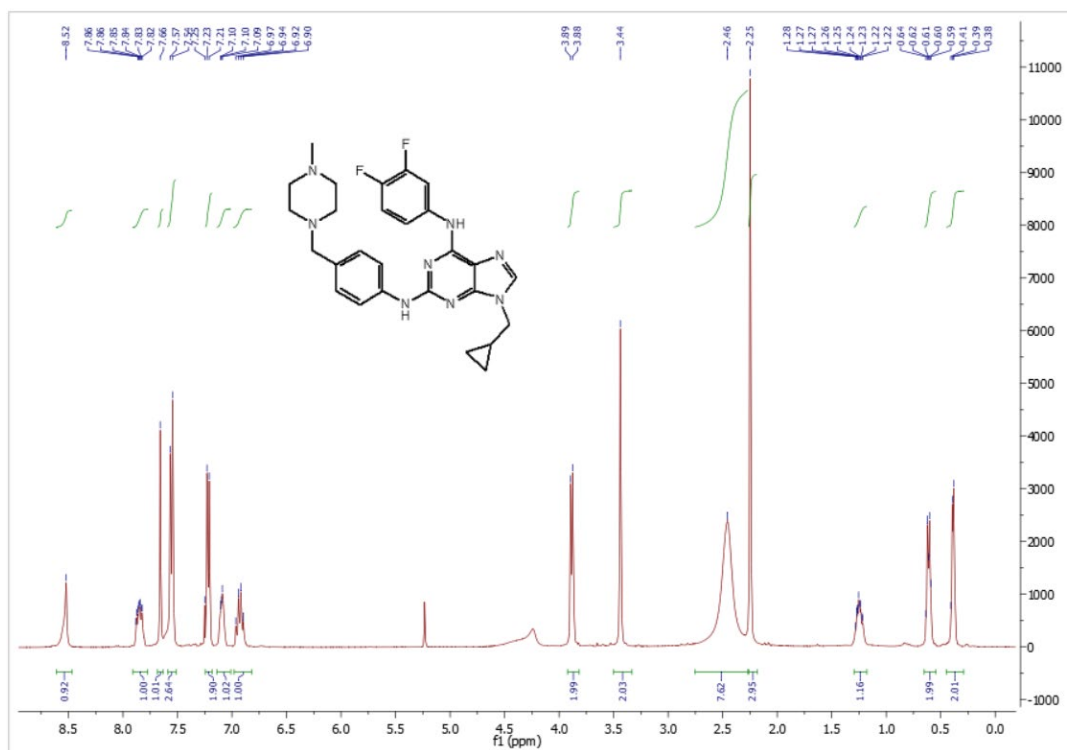
^{13}C NMR spectra of compound **7a**



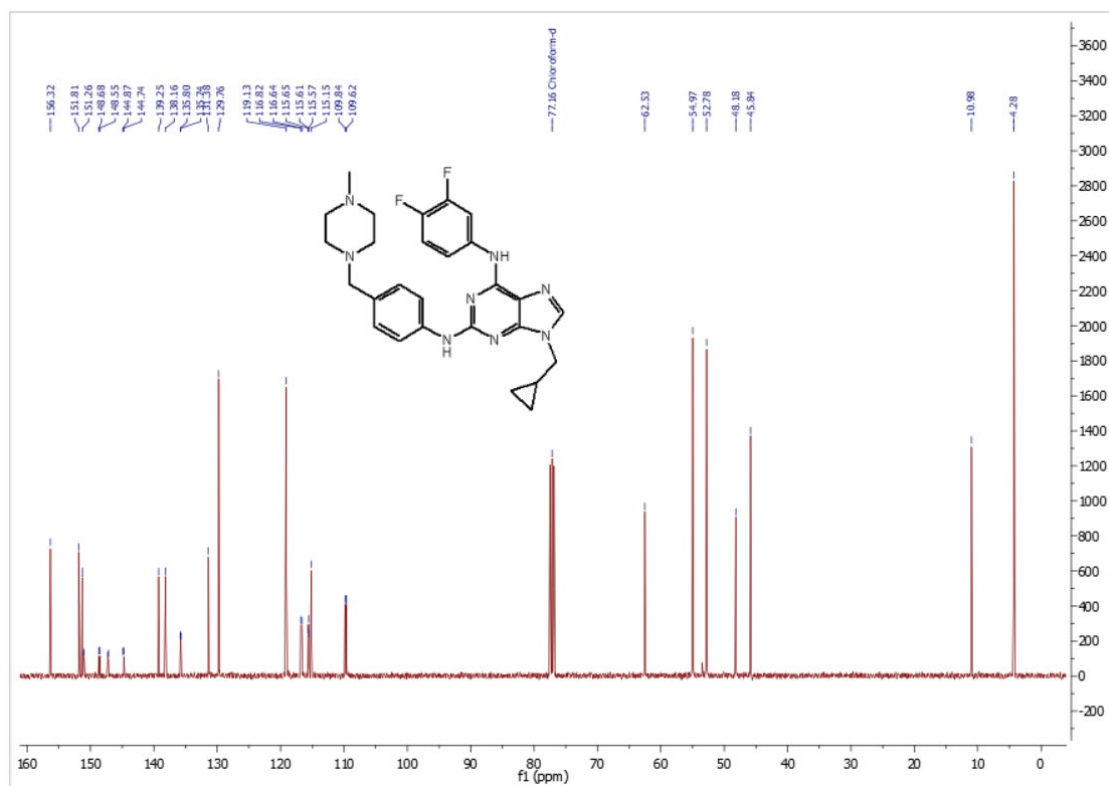
^{19}F NMR spectra of compound **7a**



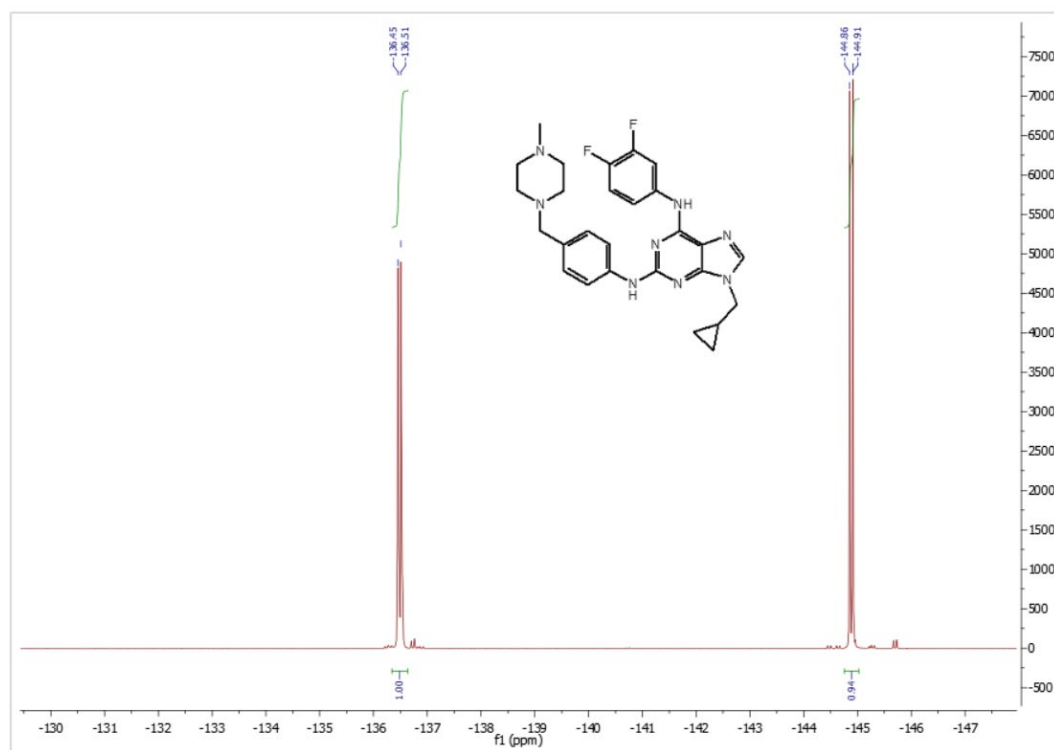
^1H NMR spectra of compound **7b**



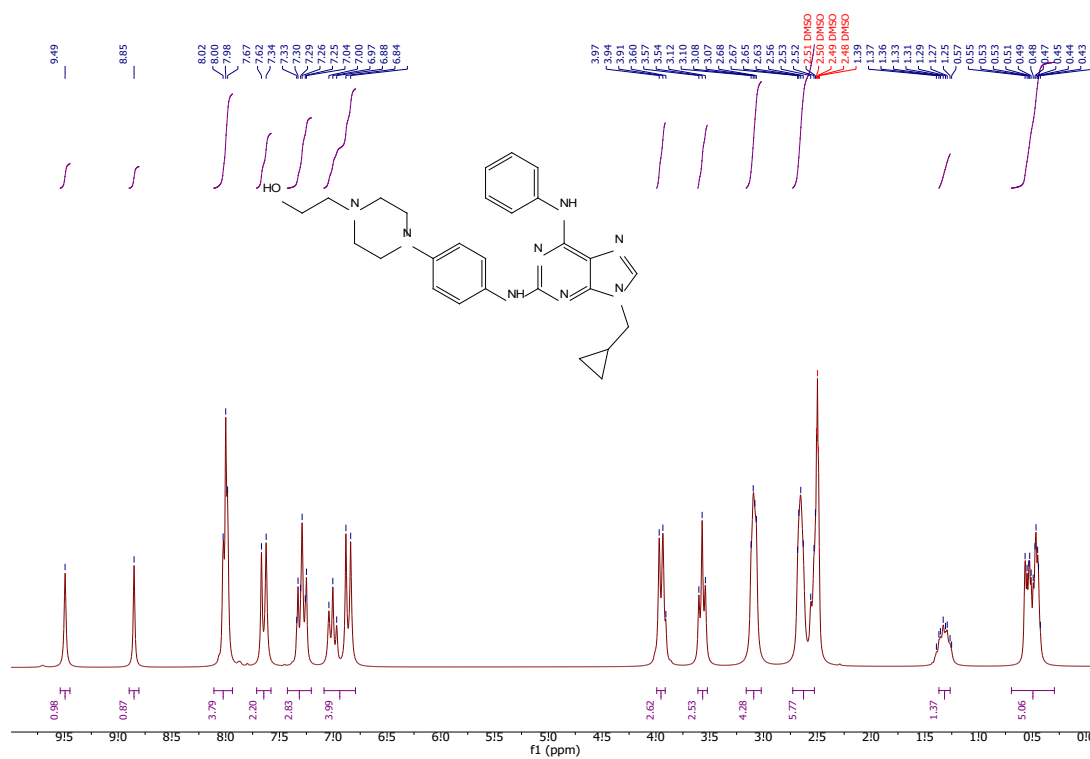
^{13}C NMR spectra of compound **7b**



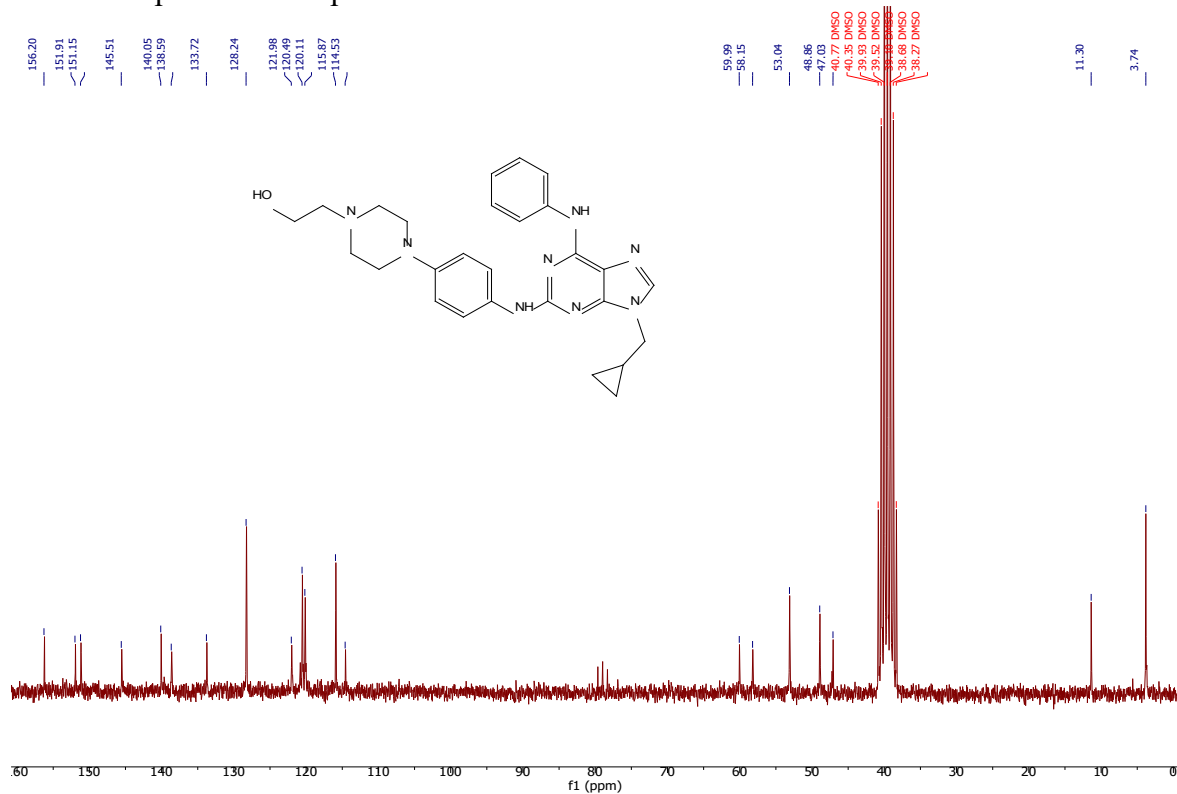
^{19}F NMR spectra of compound **7b**



¹H NMR spectra of compound **11a**

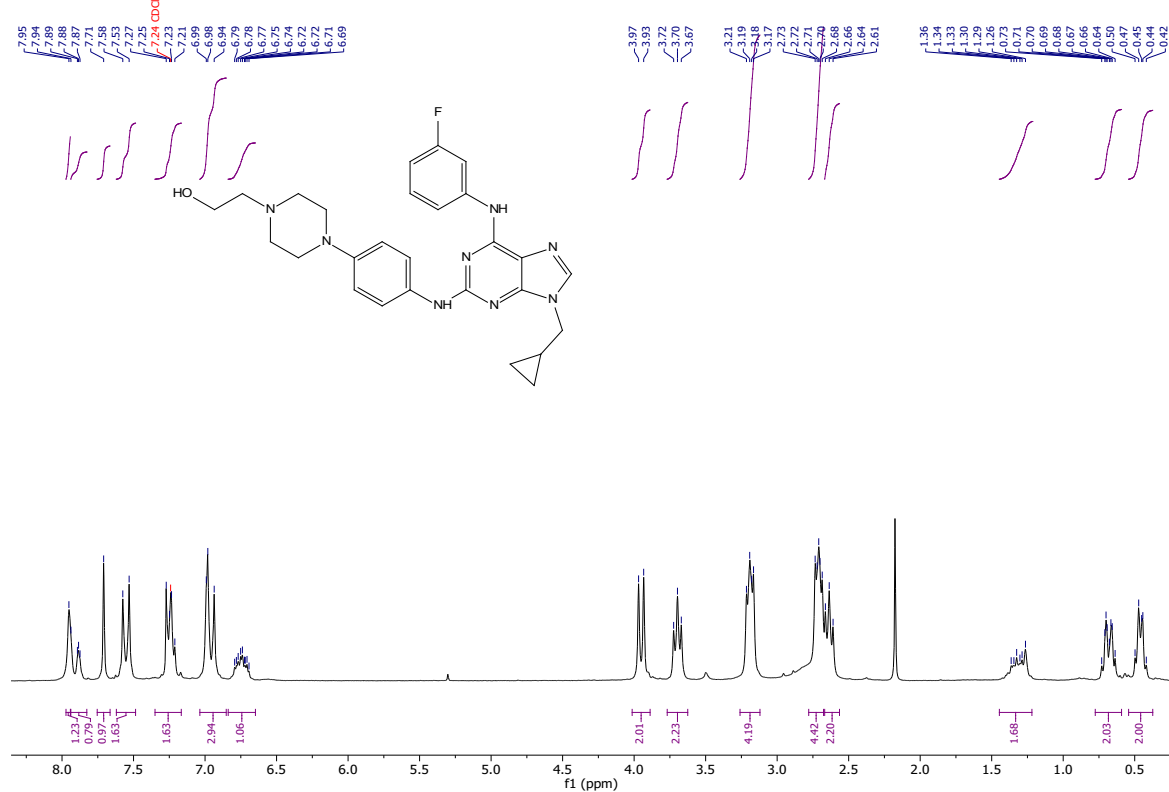


¹³C NMR spectra of compound **11a**

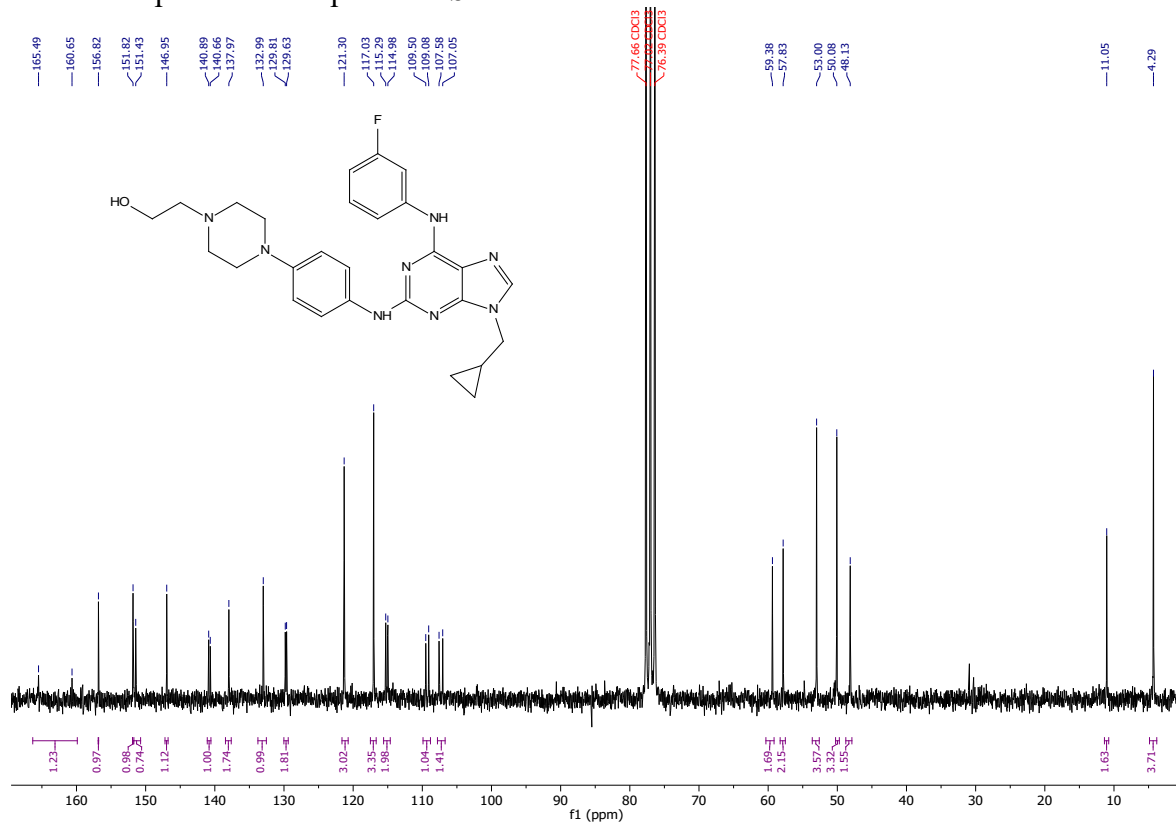


¹H NMR spectra of compound **11b**

JL.Bertrand-JL-346.1.fid



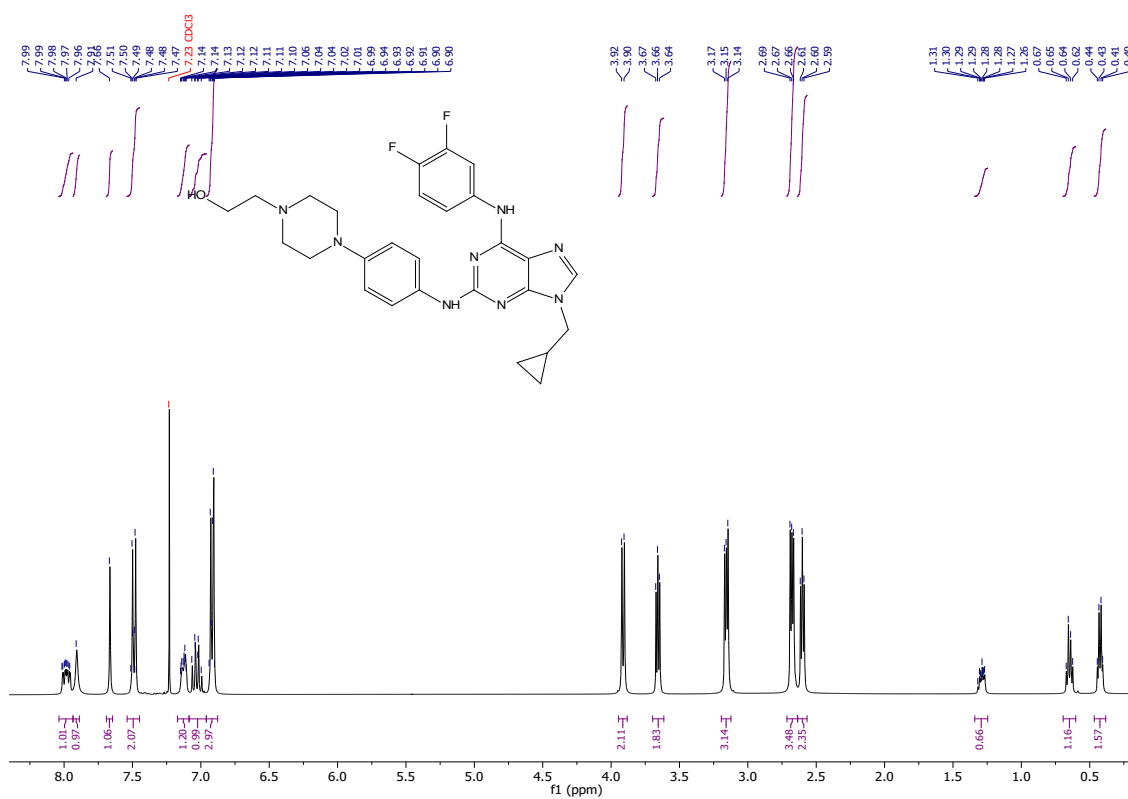
¹³C NMR spectra of compound **11b**



^{19}F NMR spectra of compound **11b**



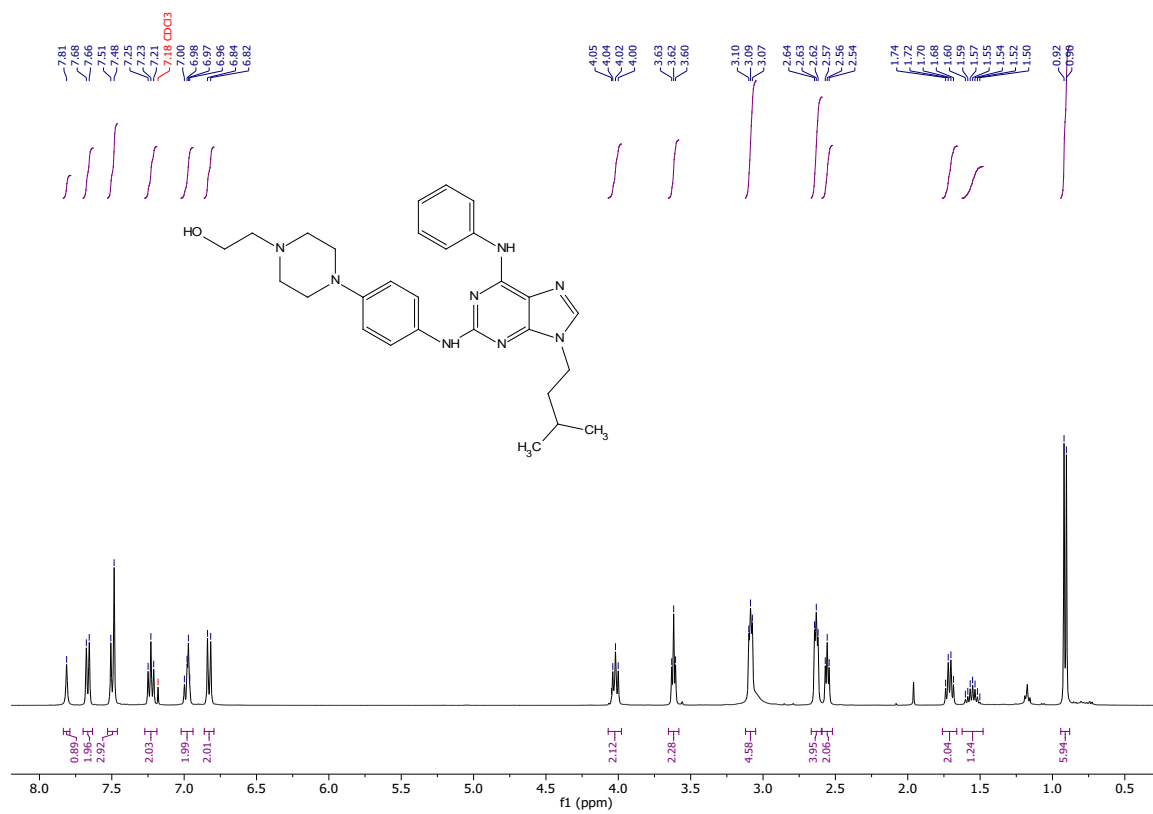
^1H NMR spectra of compound **11c**



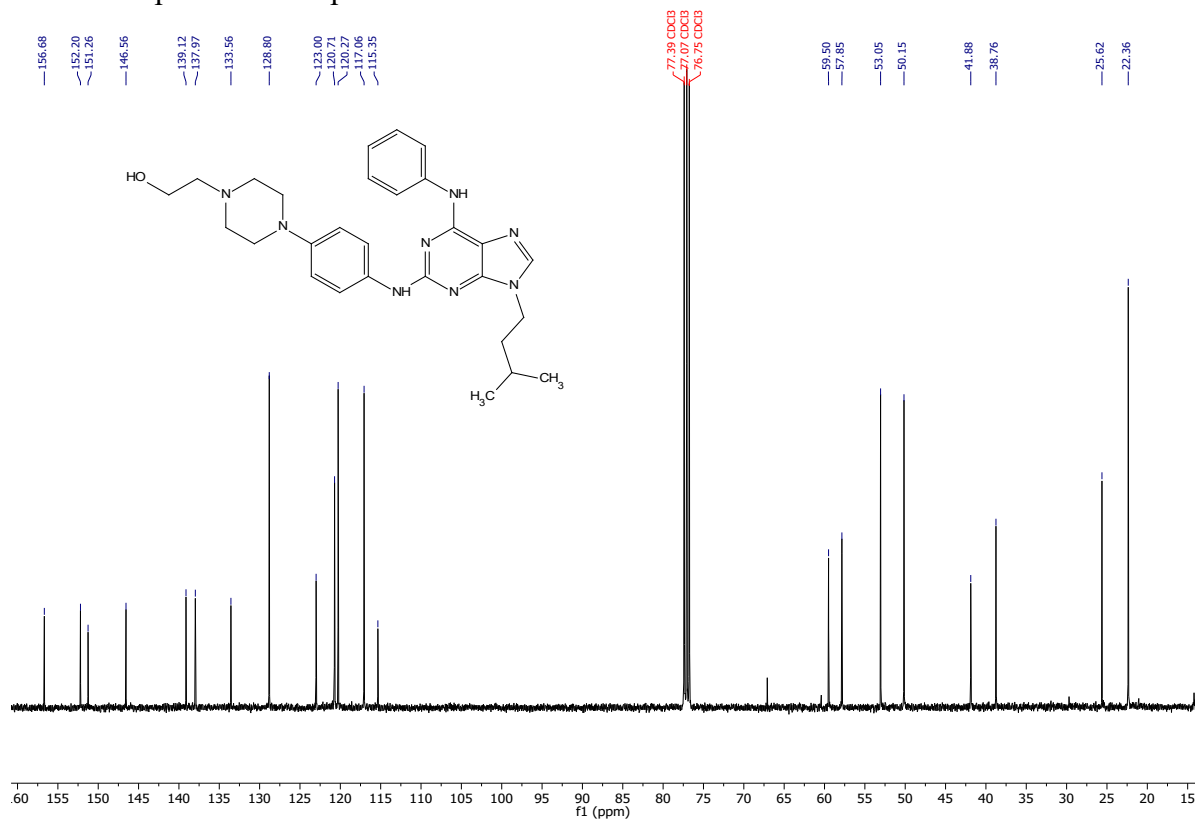
Chemical structure of compound 11c is shown above the corresponding ¹³C NMR spectrum (Figure S10). The spectrum displays peaks in the aromatic region (100-160 ppm) and aliphatic region (4-60 ppm). Key peaks are labeled with their chemical shifts (ppm): 158.33, 156.86, 151.73, 151.46, 148.94, 147.06, 138.00, 135.85, 135.62, 135.76, 135.75, 132.89, 121.46, 117.00, 116.44, 115.84, 115.24, 115.22, 115.19, 115.09, 114.95, 109.51, 77.35 (CDCl₃), 76.71 (CDCl₃), 59.39, 57.83, 53.00, 50.04, 48.16, 11.06, and 4.30.

Chemical structure of the compound is shown above the spectrum. The structure is a complex molecule featuring a central benzimidazole core. It includes a 4-(2-hydroxyethyl)piperidin-1-yl group, a 2,6-difluorophenyl group, and a 2-(cyclopropylmethyl) group. The spectrum displays two main signals: a sharp peak at approximately 136 ppm (labeled 136.10 and 136.16) and a sharp peak at approximately 145 ppm (labeled 144.98 and 145.04). The x-axis is labeled 'f1 (ppm)' and ranges from -133 to -149.

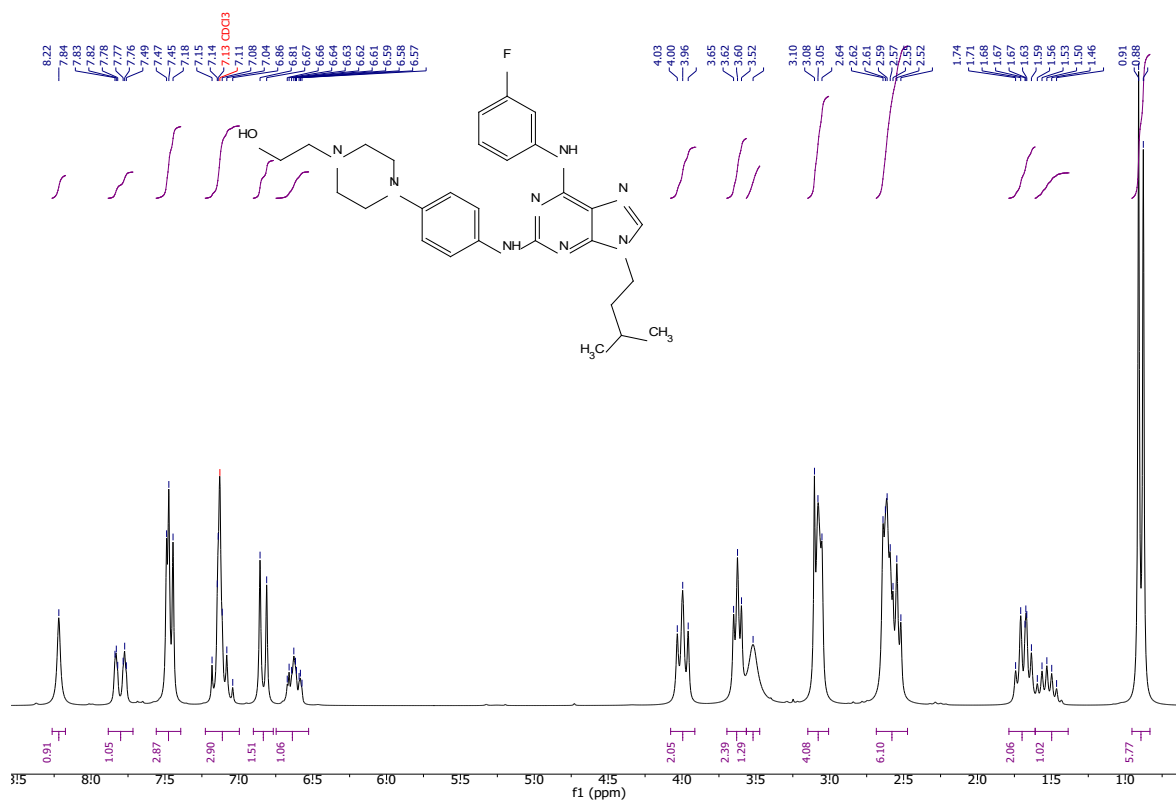
¹H NMR spectra of compound **11d**



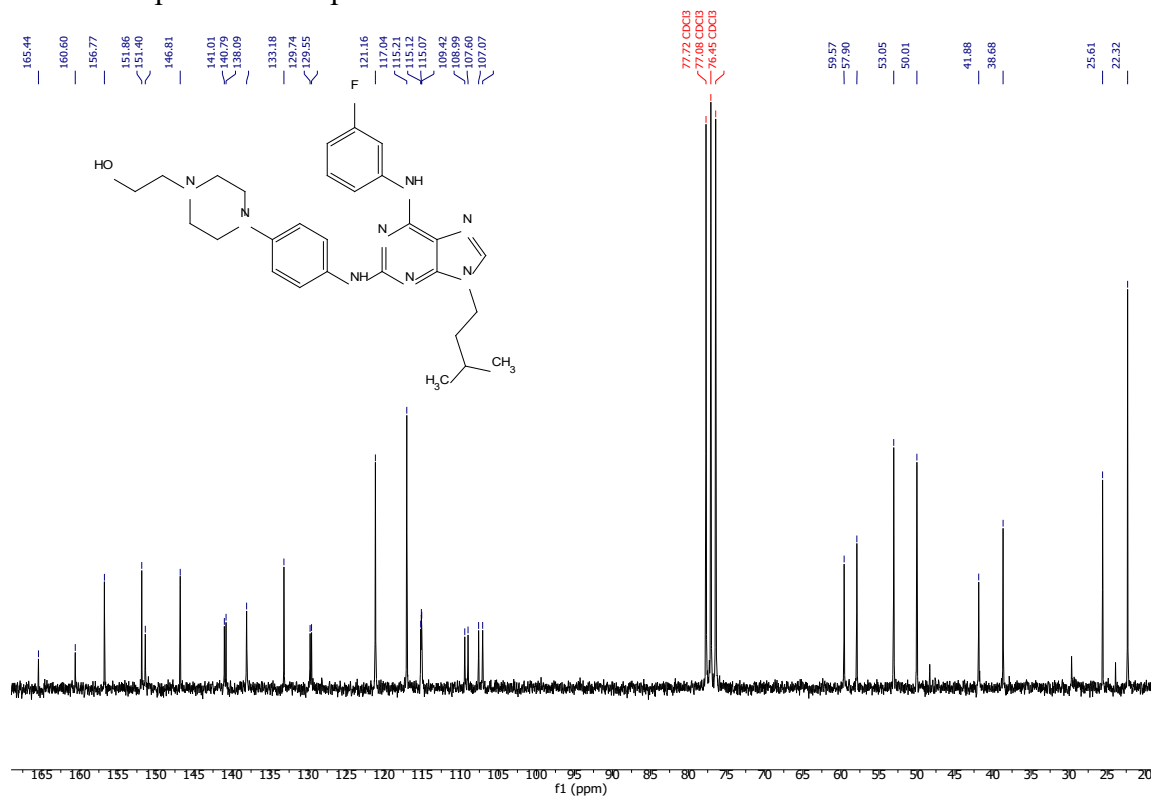
¹³C NMR spectra of compound **11d**



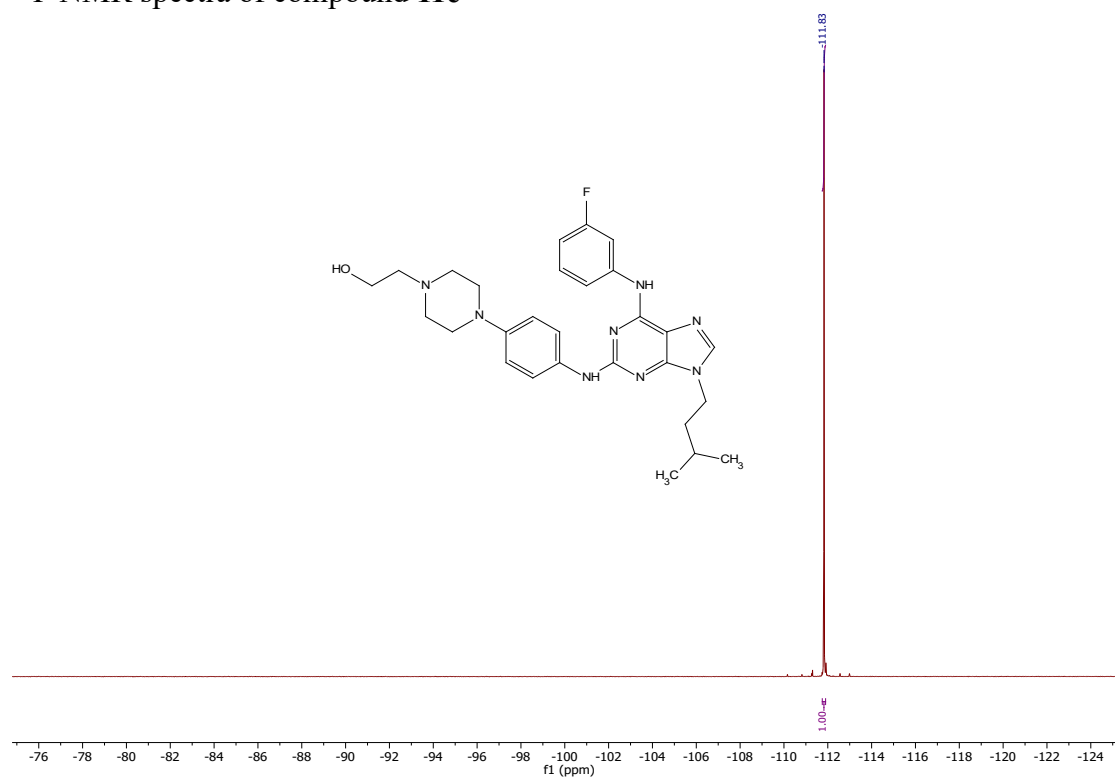
¹H NMR spectra of compound 11e



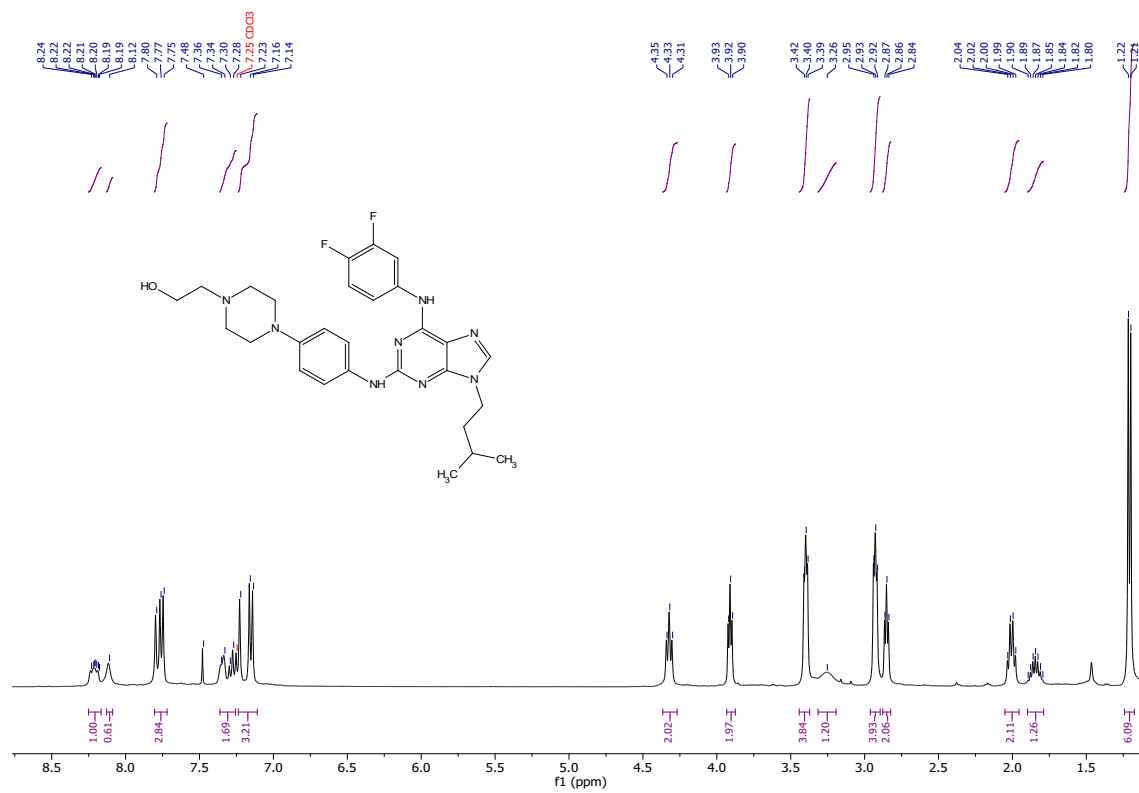
¹³C NMR spectra of compound 11e



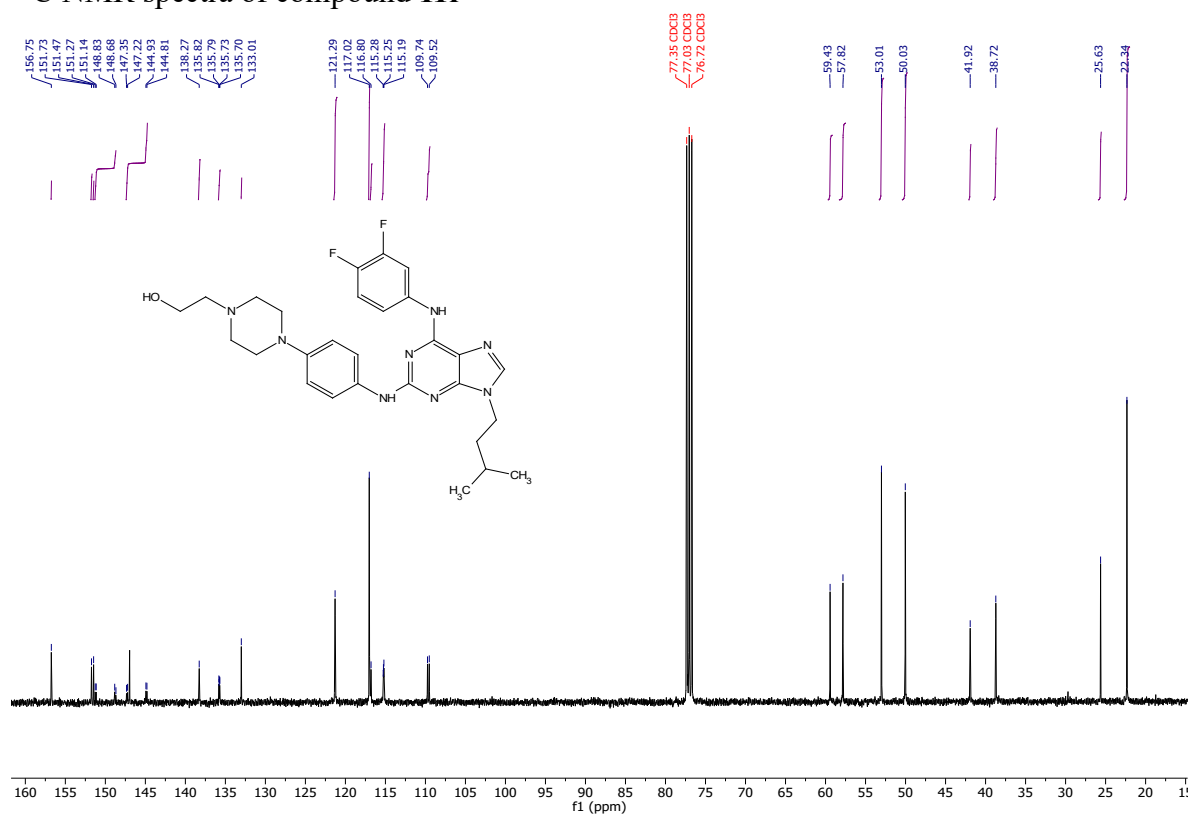
^{19}F NMR spectra of compound **11e**



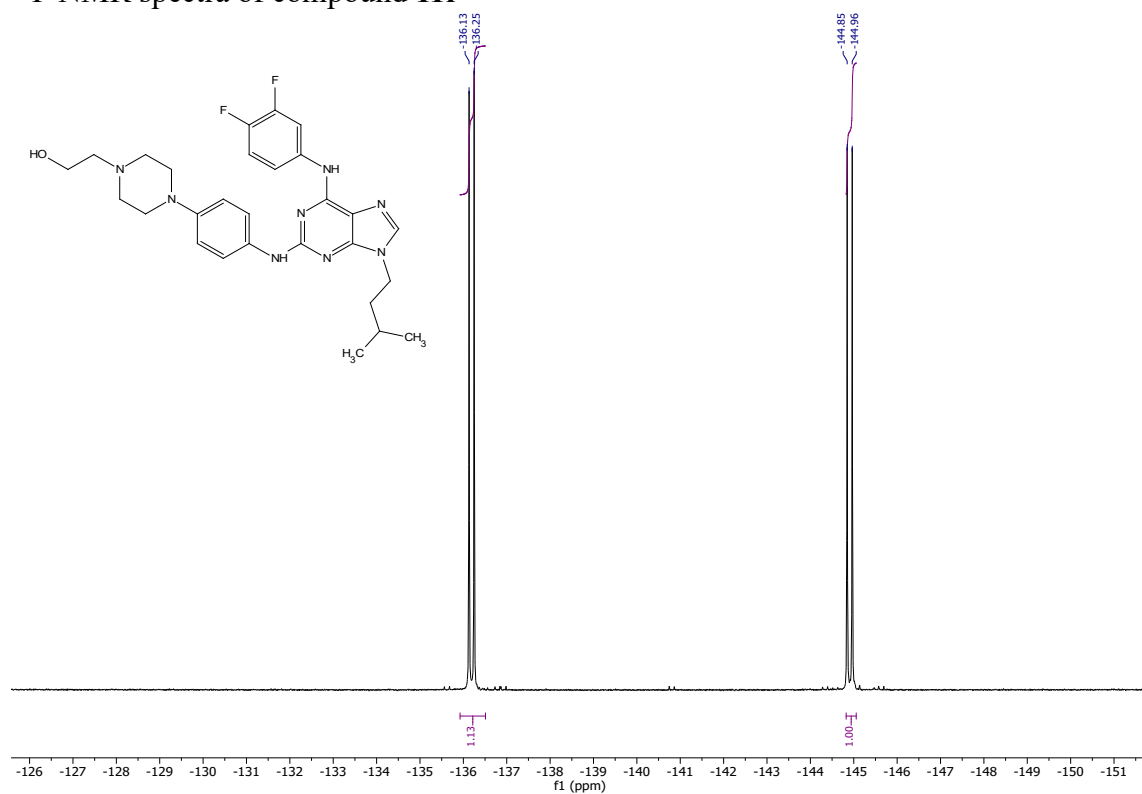
^1H NMR spectra of compound **11f**



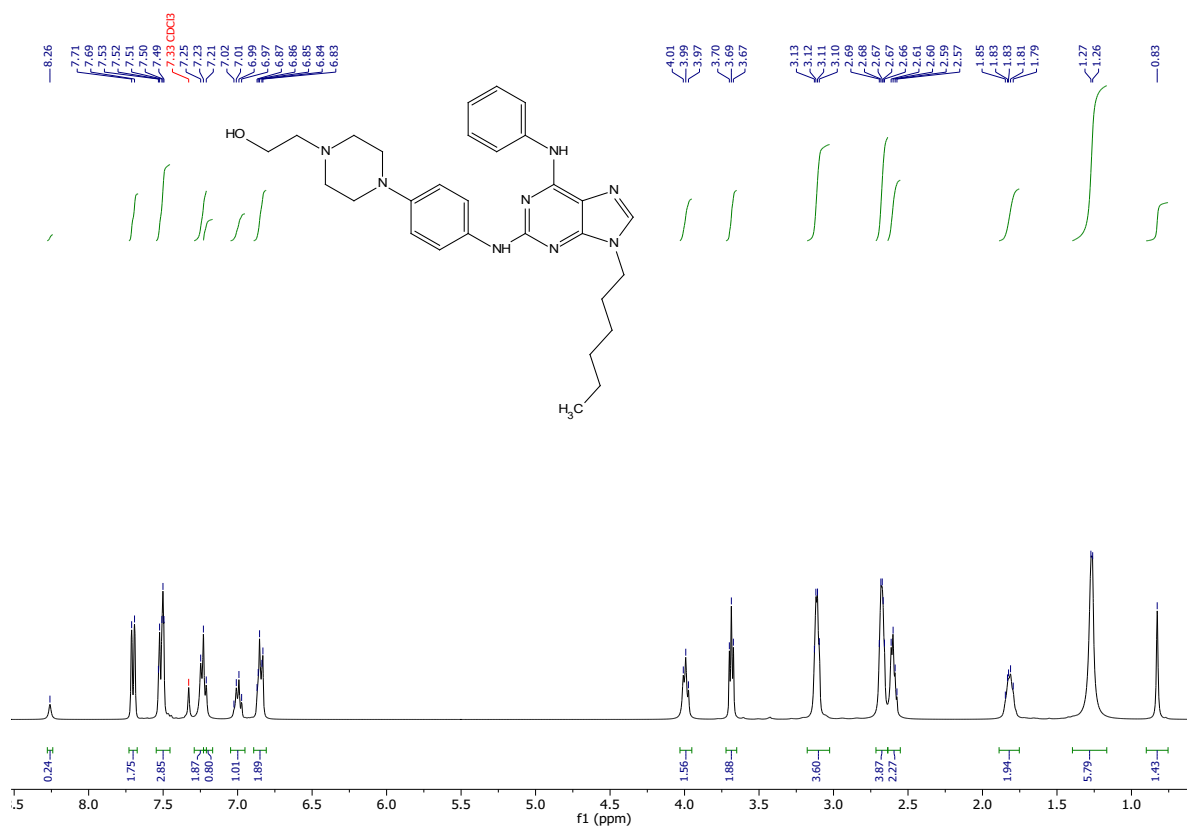
¹³C NMR spectra of compound **11f**



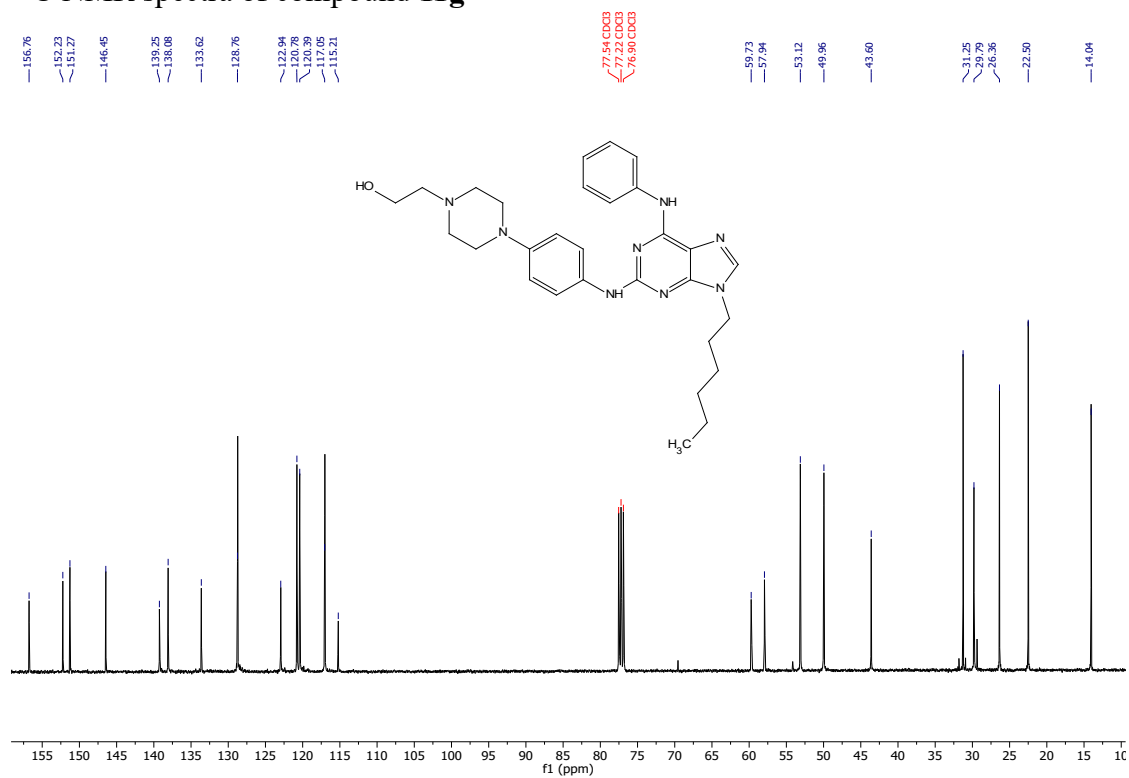
¹⁹F NMR spectra of compound **11f**



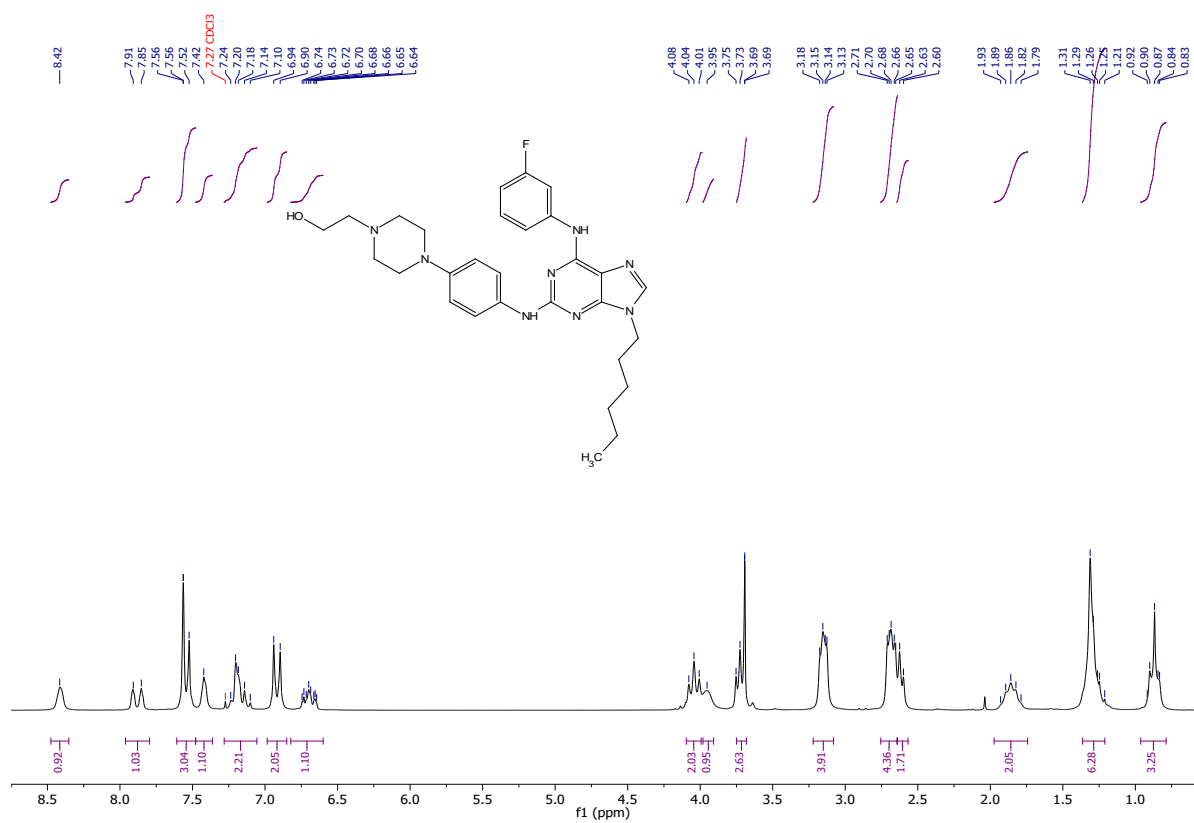
¹H NMR spectra of compound **11g**



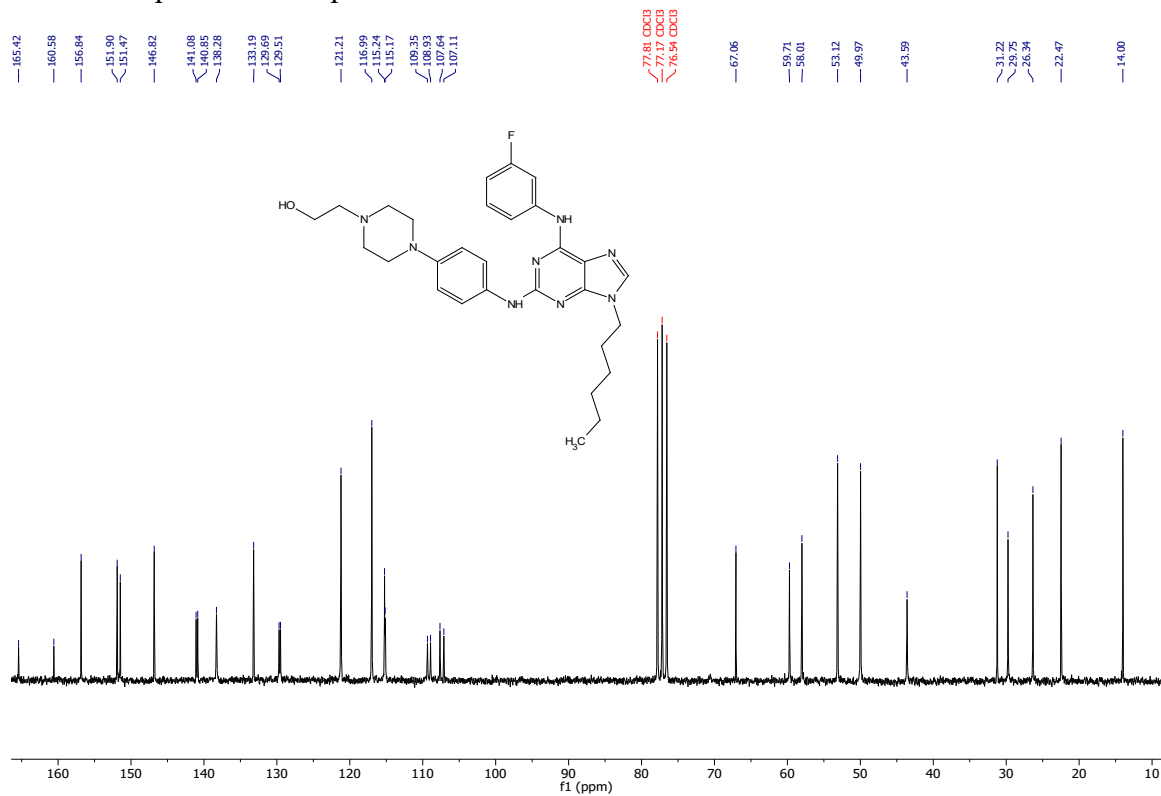
¹³C NMR spectra of compound **11g**



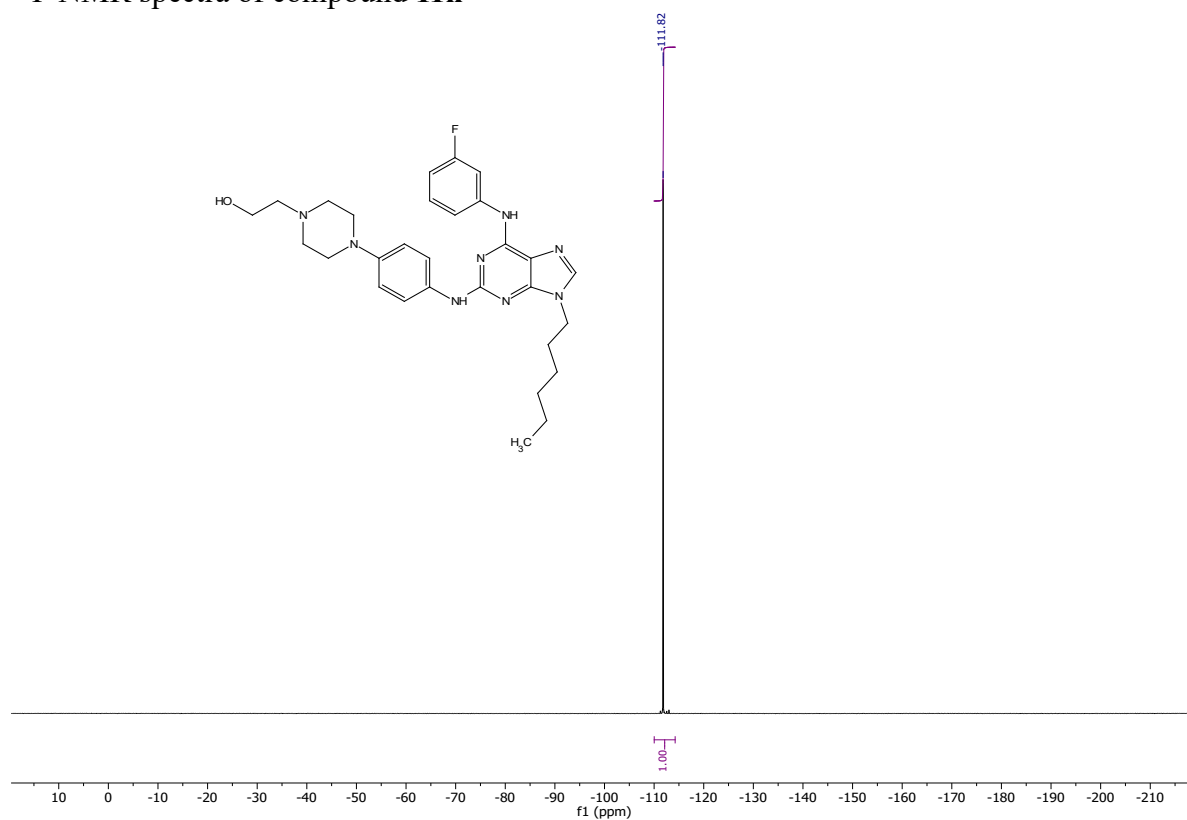
¹H NMR spectra of compound **11h**



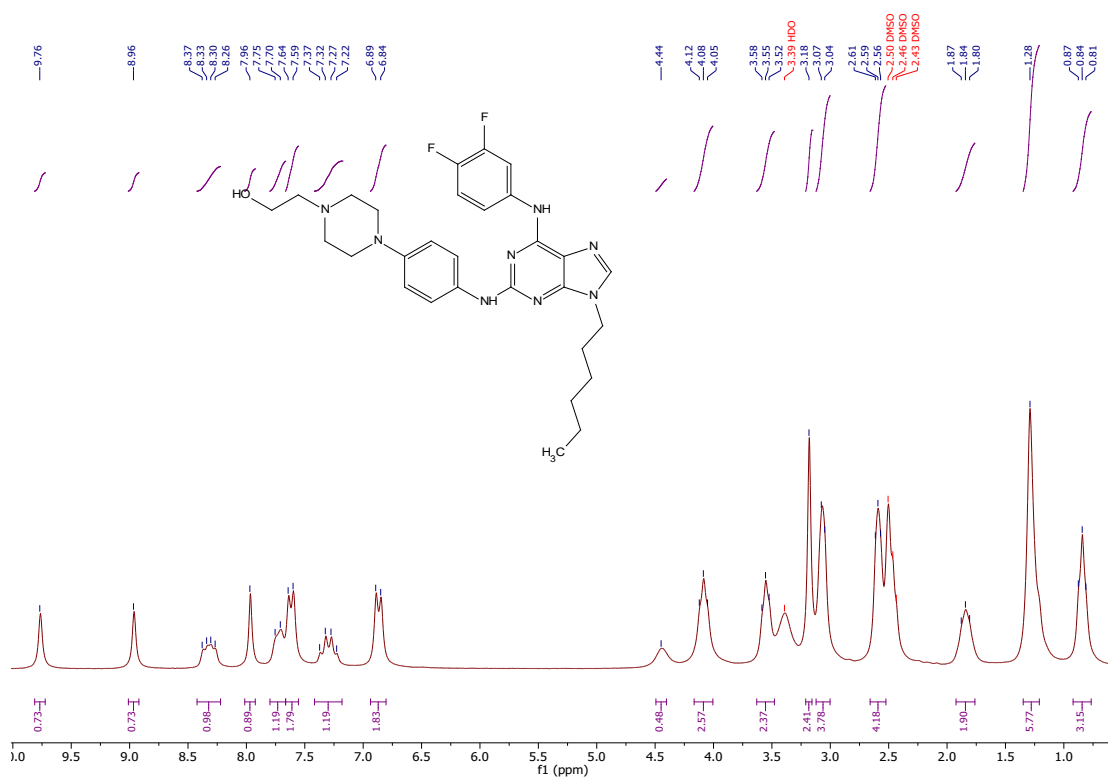
¹³C NMR spectra of compound **11h**



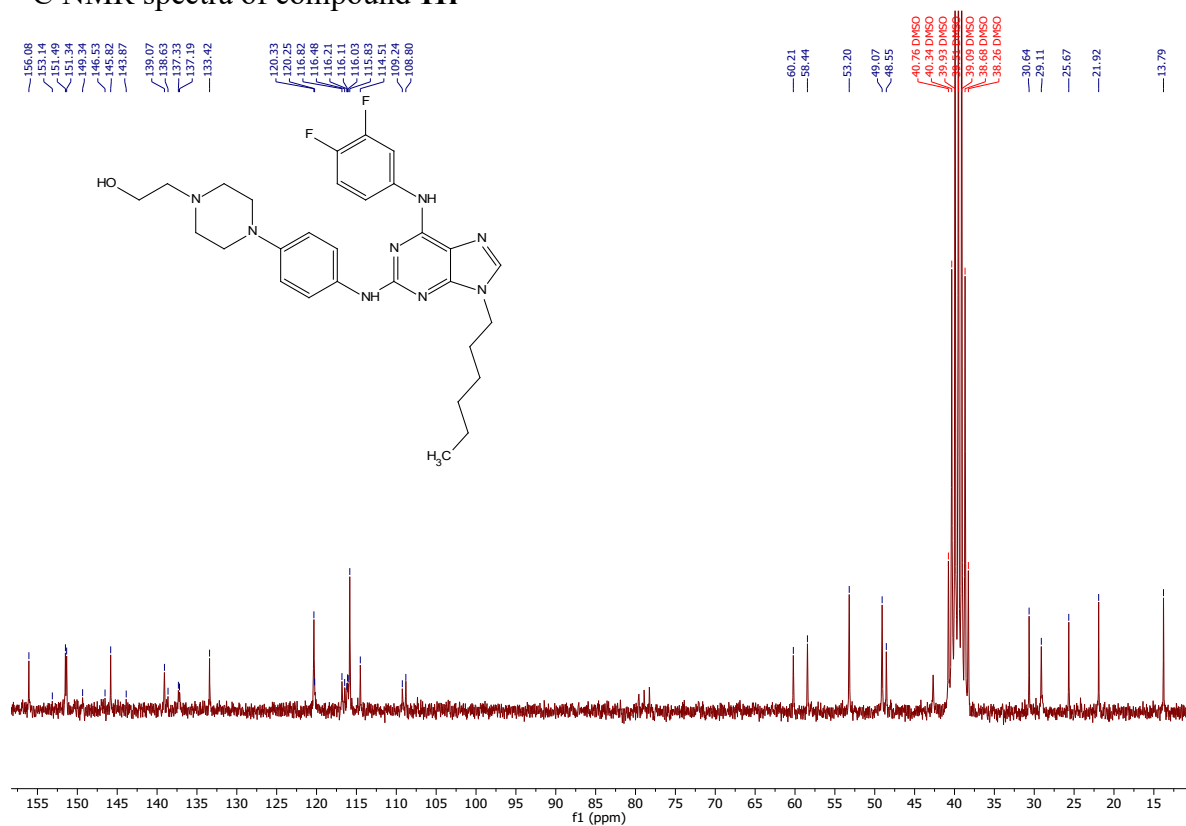
¹⁹F NMR spectra of compound **11h**



¹H NMR spectra of compound **11i**

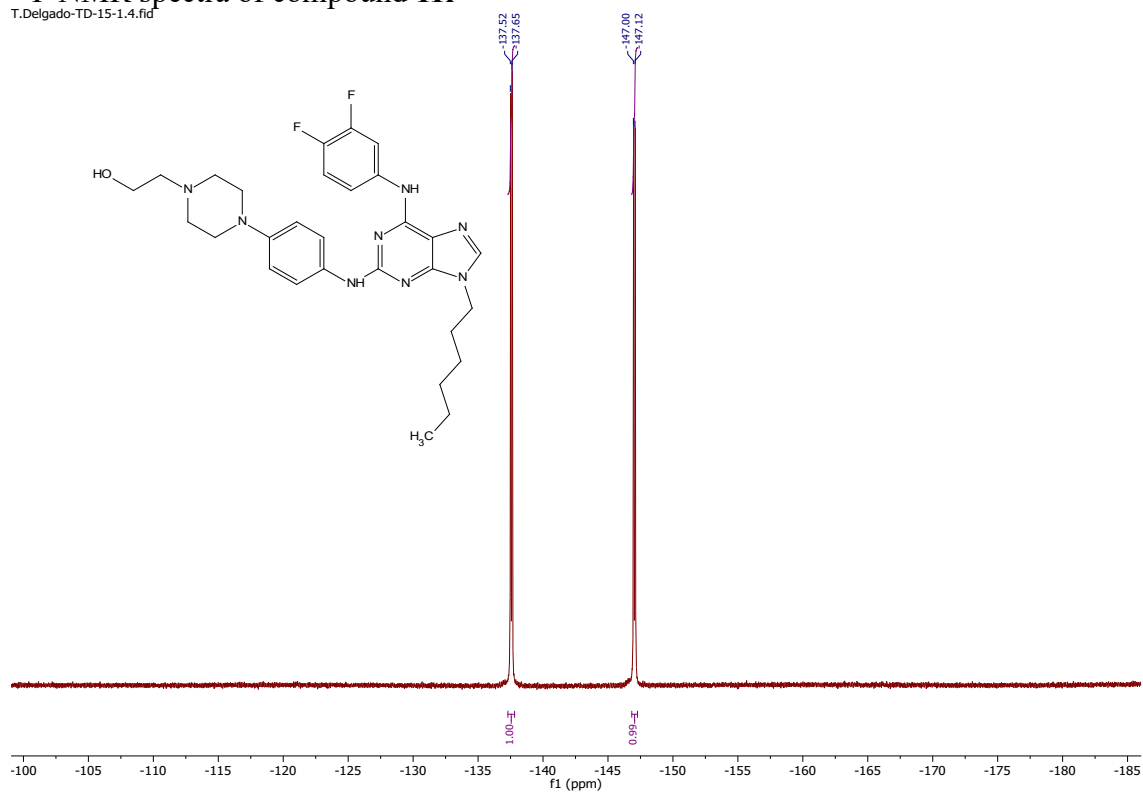


¹³C NMR spectra of compound **11i**

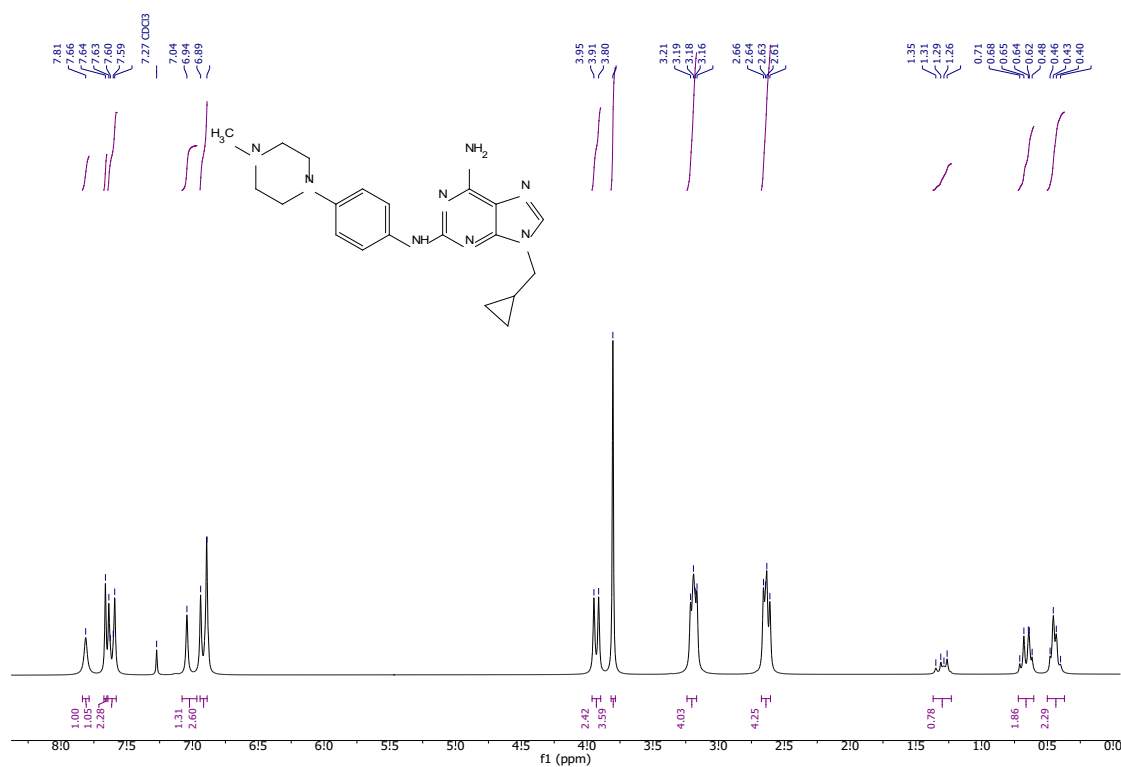


¹⁹F NMR spectra of compound **11i**

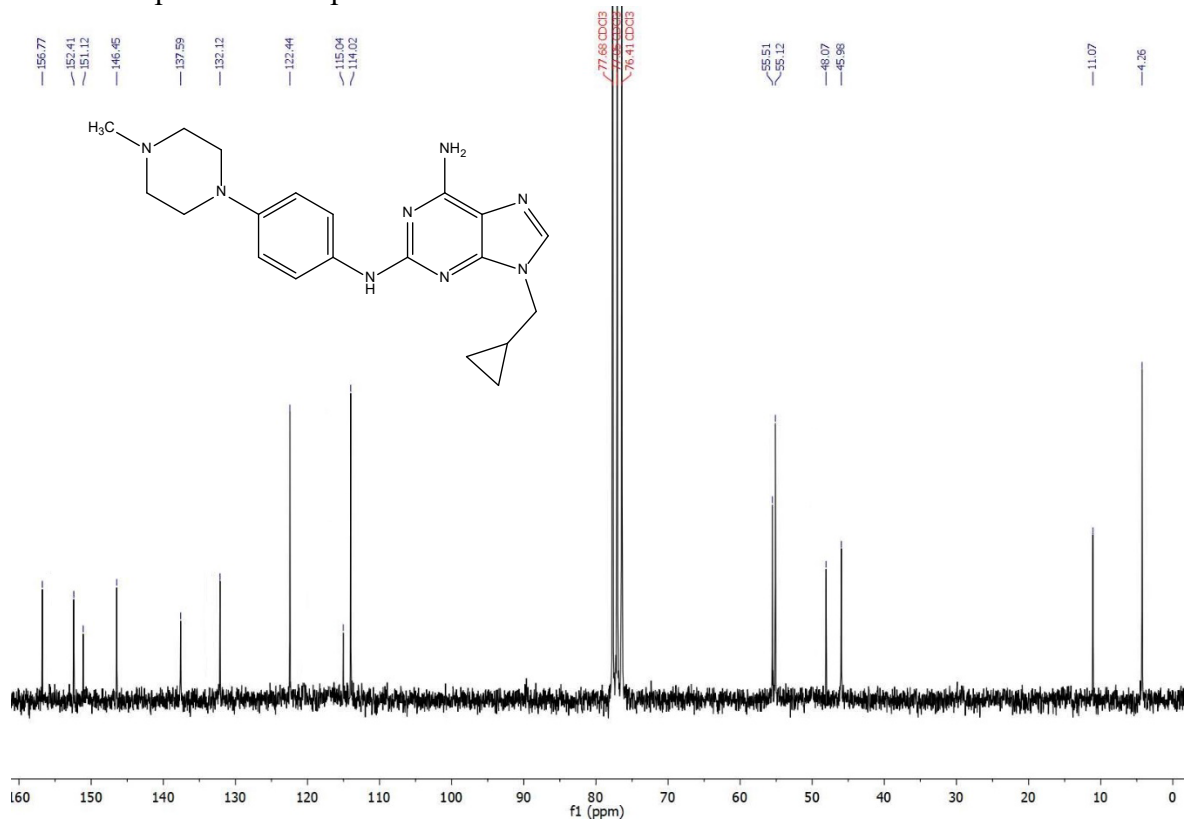
T.Delgado-TD-15-1.4.fid



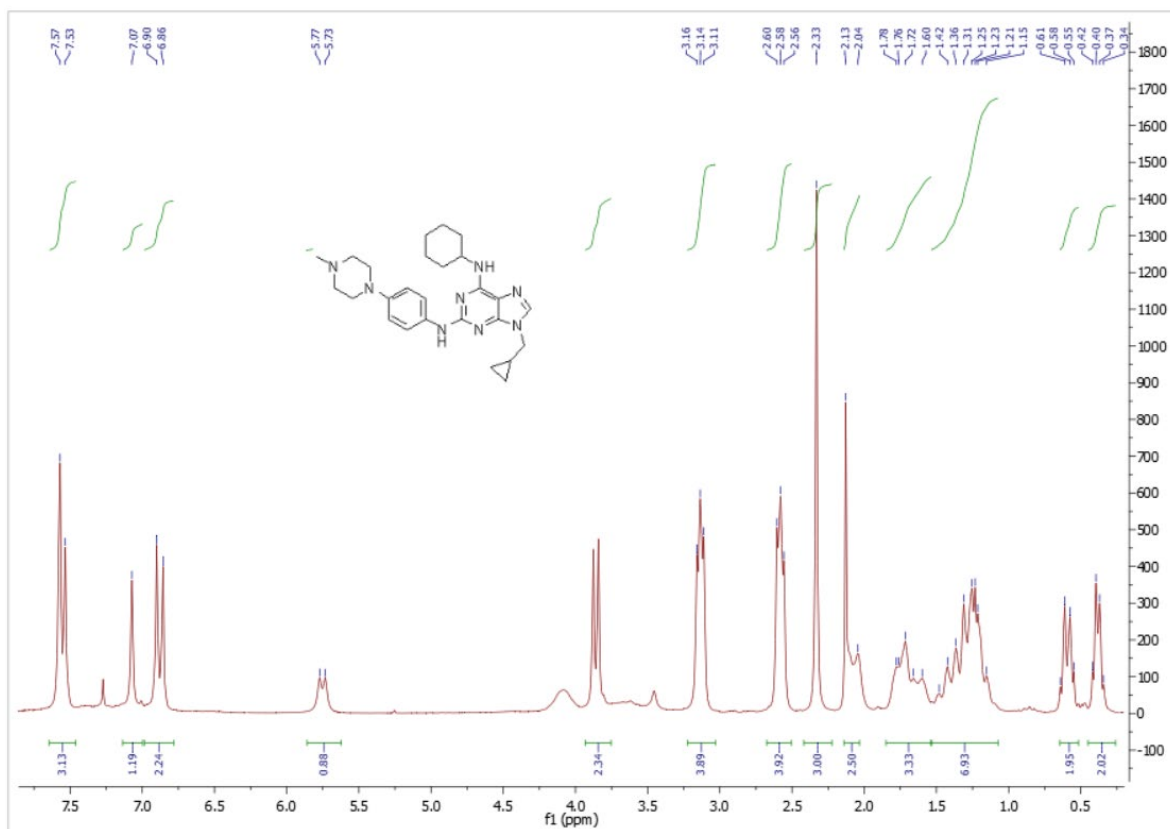
¹H NMR spectra of compound **13a**



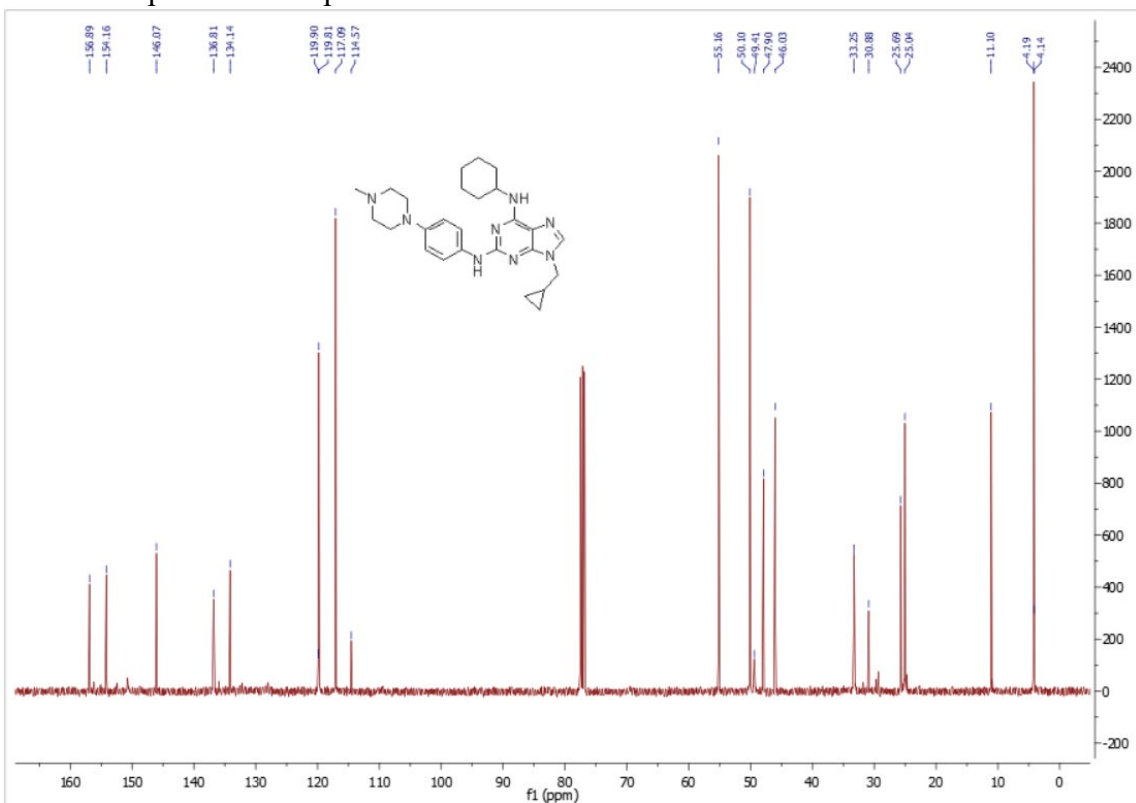
¹³C NMR spectra of compound **13b**



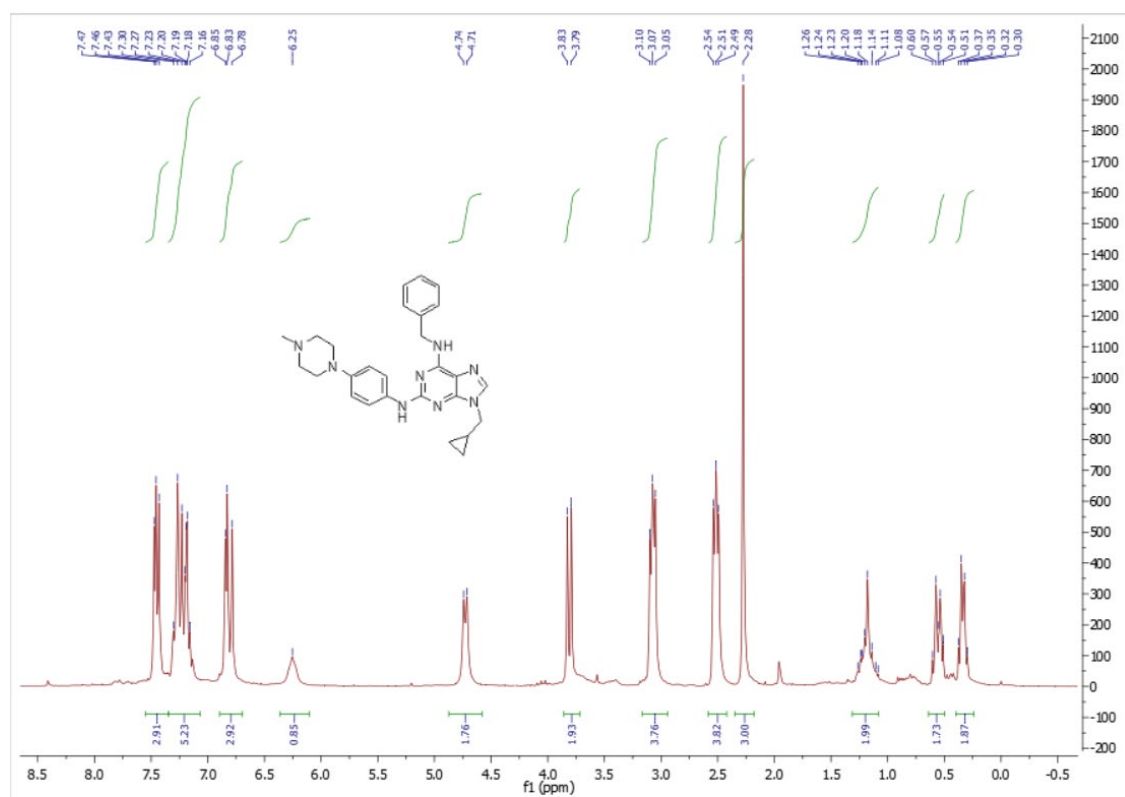
¹H NMR spectra of compound **13b**



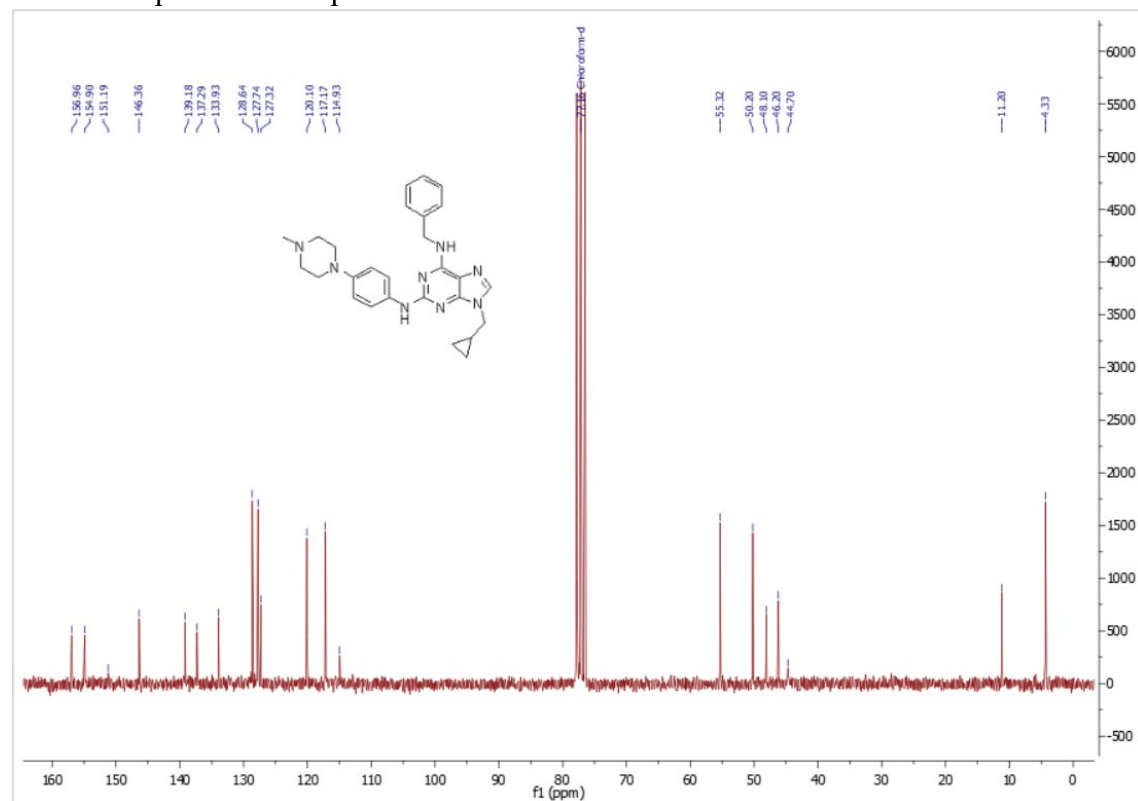
¹³C NMR spectra of compound **13b**



¹H NMR spectra of compound **13c**



¹³C NMR spectra of compound **13c**

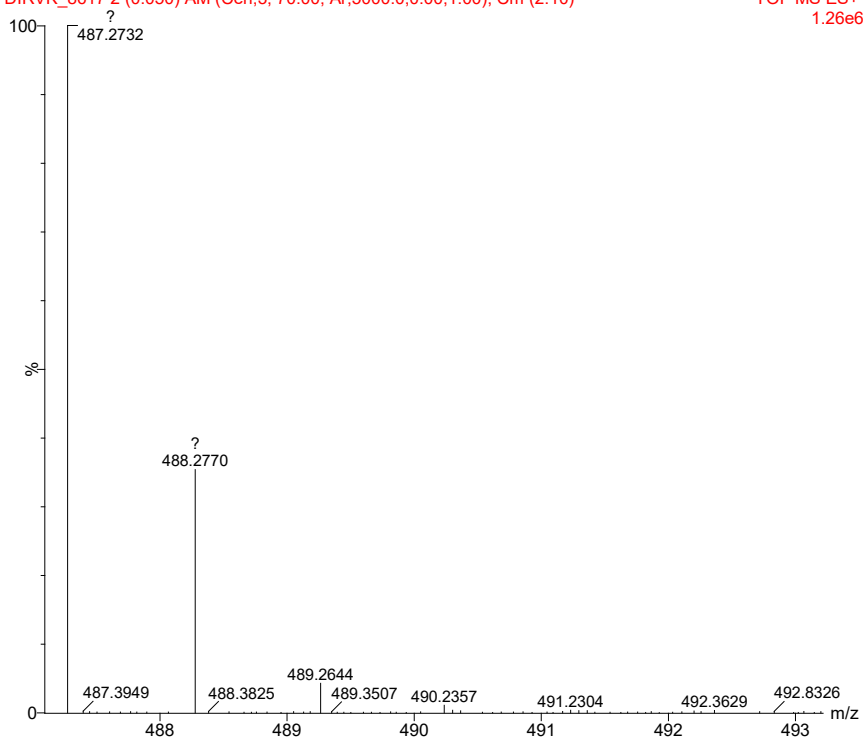


Mass spectra of compound 7a

direct infusion latky VK

DIRVK_8617 2 (0.050) AM (Cen,3, 70.00, Ar,5000.0,0.00,1.00); Cm (2:10)

TOF MS ES+
1.26e6

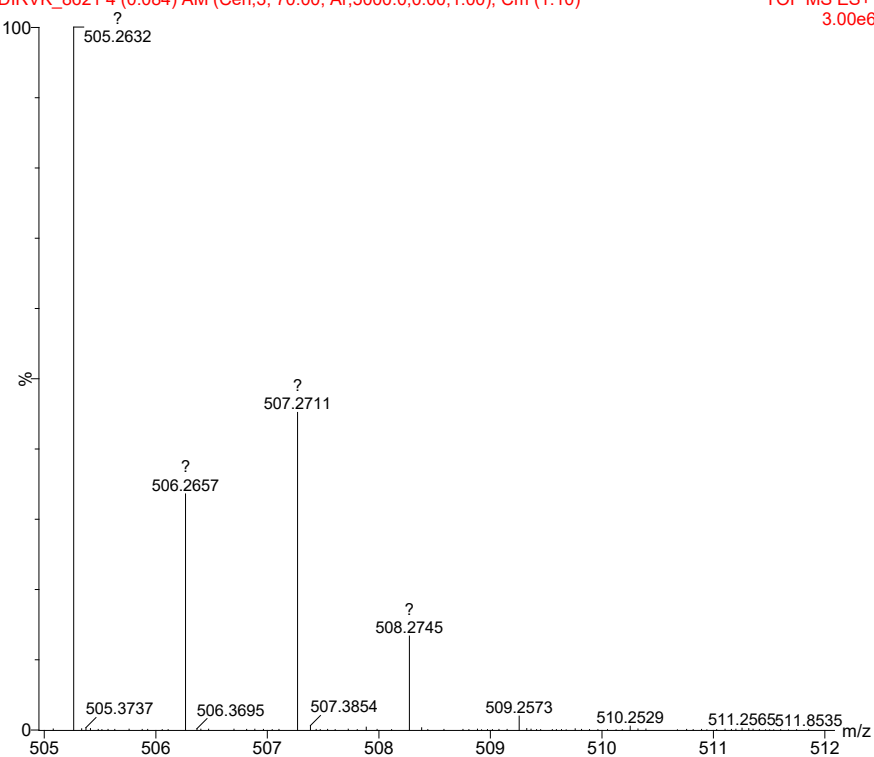


Mass spectra of compound 7b

direct infusion latky VK

DIRVK_8621 4 (0.084) AM (Cen,3, 70.00, Ar,5000.0,0.00,1.00); Cm (1:10)

TOF MS ES+
3.00e6

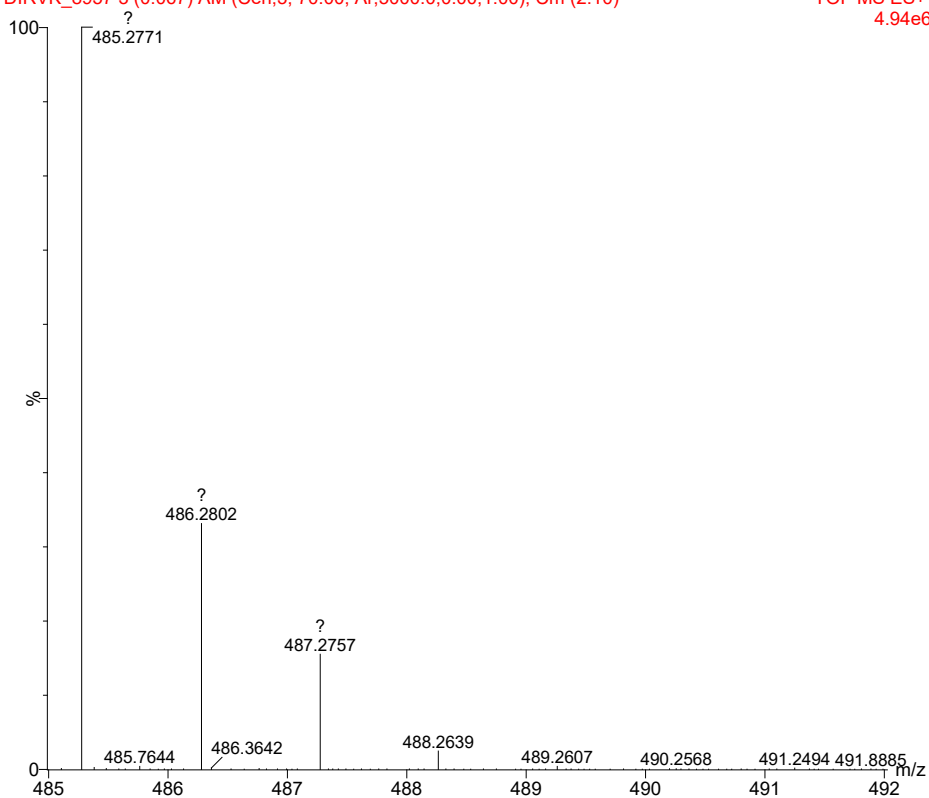


Mass spectra of compound **11a**

direct infusion latky VK

DIRVK_8957 3 (0.067) AM (Cen,3, 70.00, Ar,5000.0,0.00,1.00); Cm (2:10)

TOF MS ES+
4.94e6

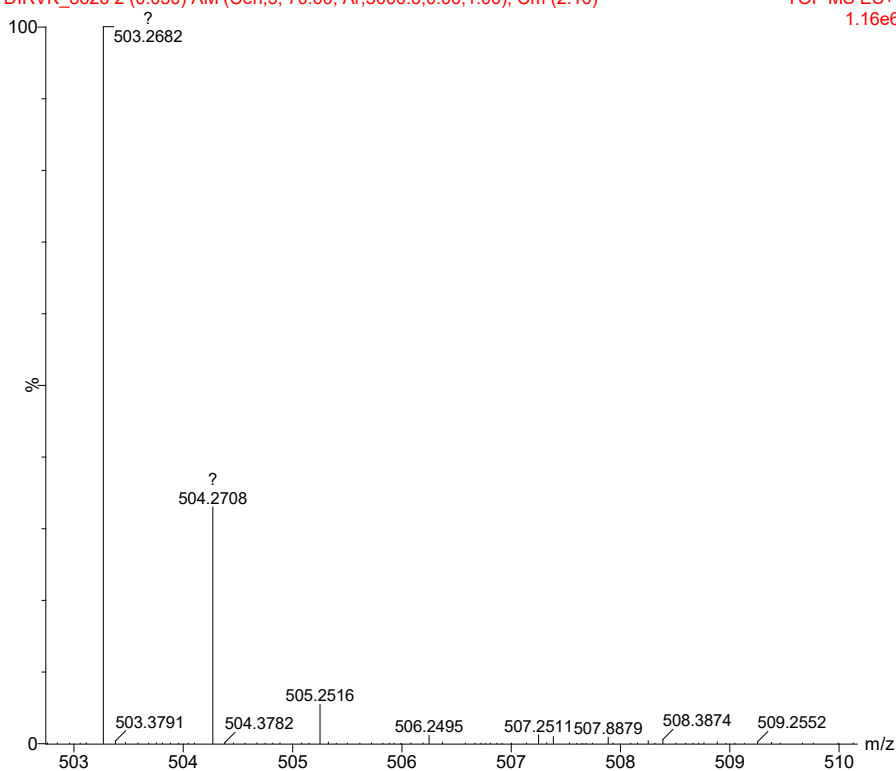


Mass spectra of compound **11b**

direct infusion latky VK

DIRVK_8626 2 (0.050) AM (Cen,3, 70.00, Ar,5000.0,0.00,1.00); Cm (2:10)

TOF MS ES+
1.16e6

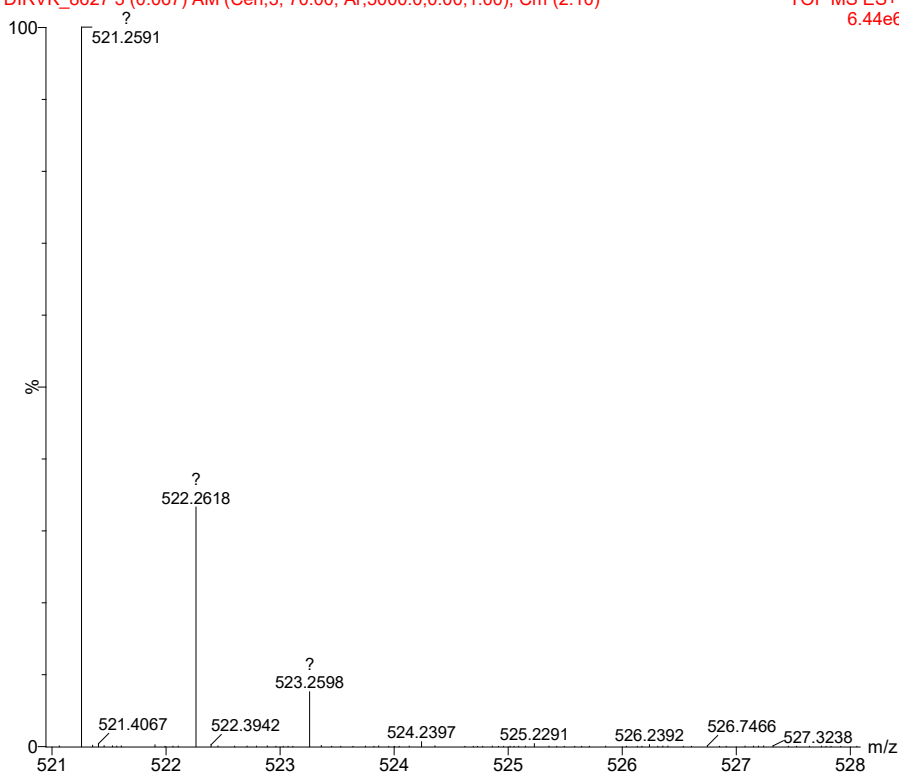


Mass spectra of compound 11c

direct infusion latky VK

DIRVK_8627 3 (0.067) AM (Cen,3, 70.00, Ar,5000.0,0.00,1.00); Cm (2:10)

TOF MS ES+
6.44e6

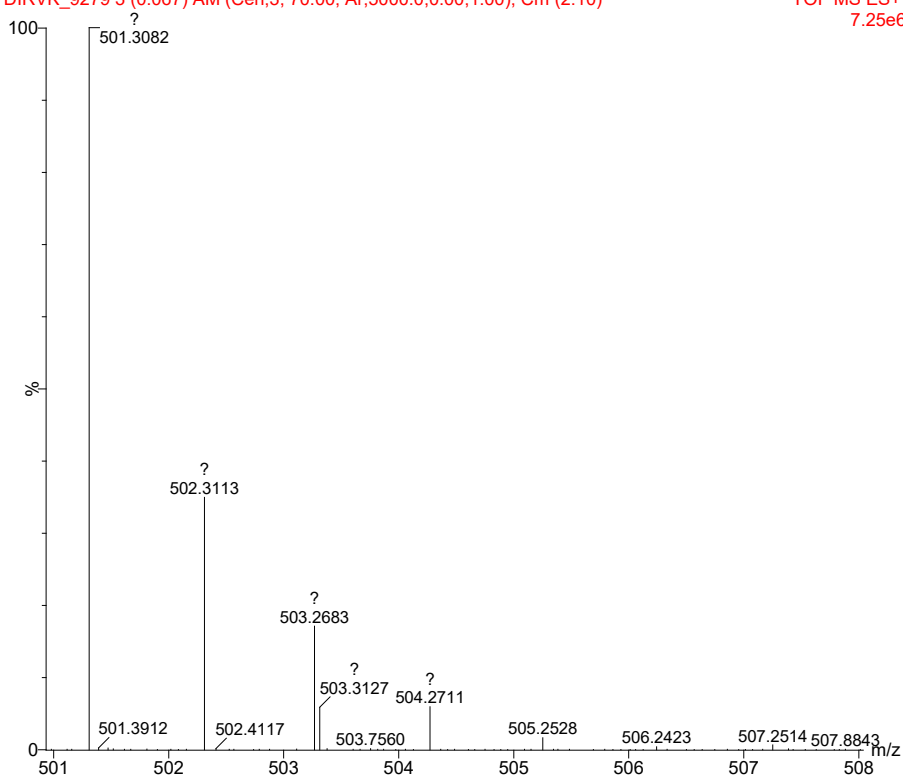


Mass spectra of compound 11d

direct infusion latky VK

DIRVK_9279 3 (0.067) AM (Cen,3, 70.00, Ar,5000.0,0.00,1.00); Cm (2:10)

TOF MS ES+
7.25e6

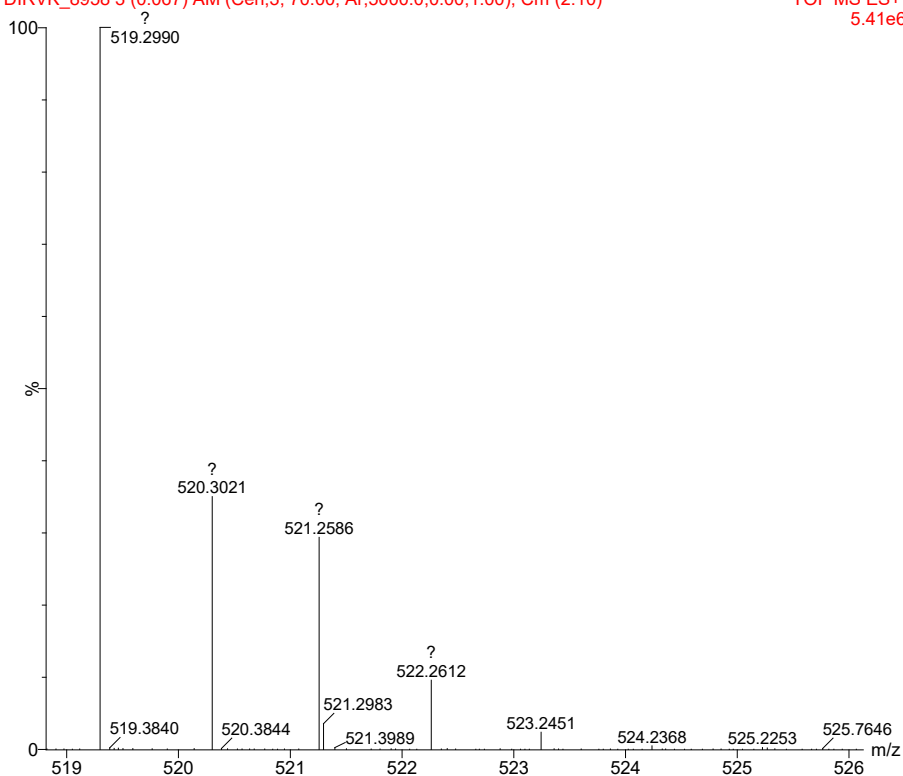


Mass spectra of compound **11e**

direct infusion latky VK

DIRVK_8958 3 (0.067) AM (Cen,3, 70.00, Ar,5000.0,0.00,1.00); Cm (2:10)

TOF MS ES+
5.41e6



Mass spectra of compound **11f**

direct infusion latky VK

DIRVK_9268 4 (0.084) AM (Cen,3, 70.00, Ar,5000.0,0.00,1.00); Cm (2:10)

TOF MS ES+
4.21e6

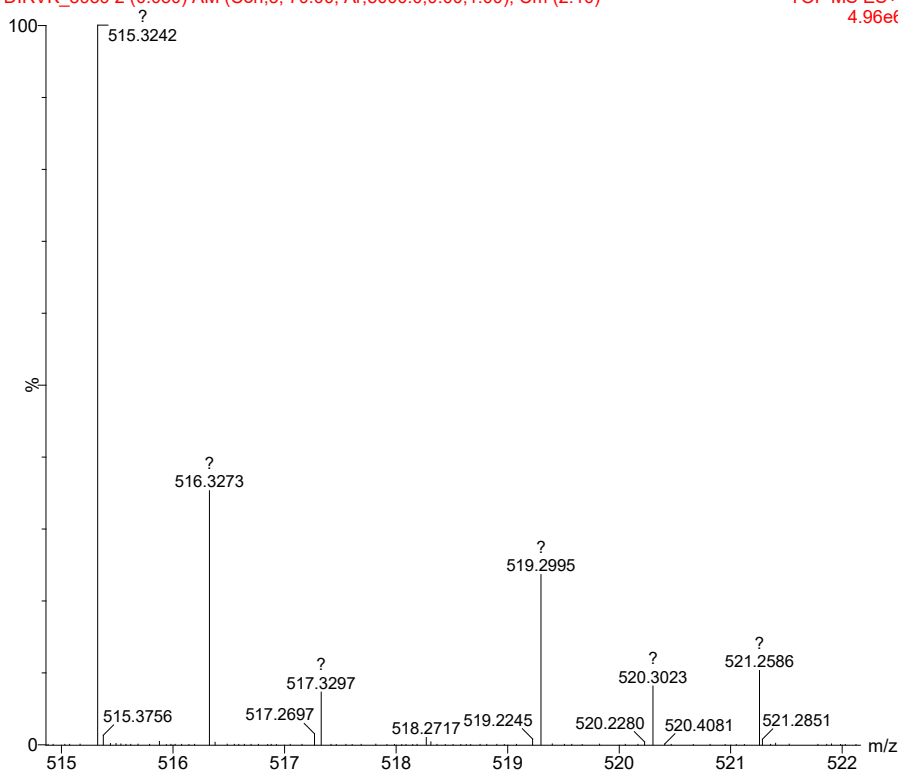


Mass spectra of compound 11g

direct infusion latky VK

DIRVK_8959 2 (0.050) AM (Cen,3, 70.00, Ar,5000.0,0.00,1.00); Cm (2:10)

TOF MS ES+
4.96e6

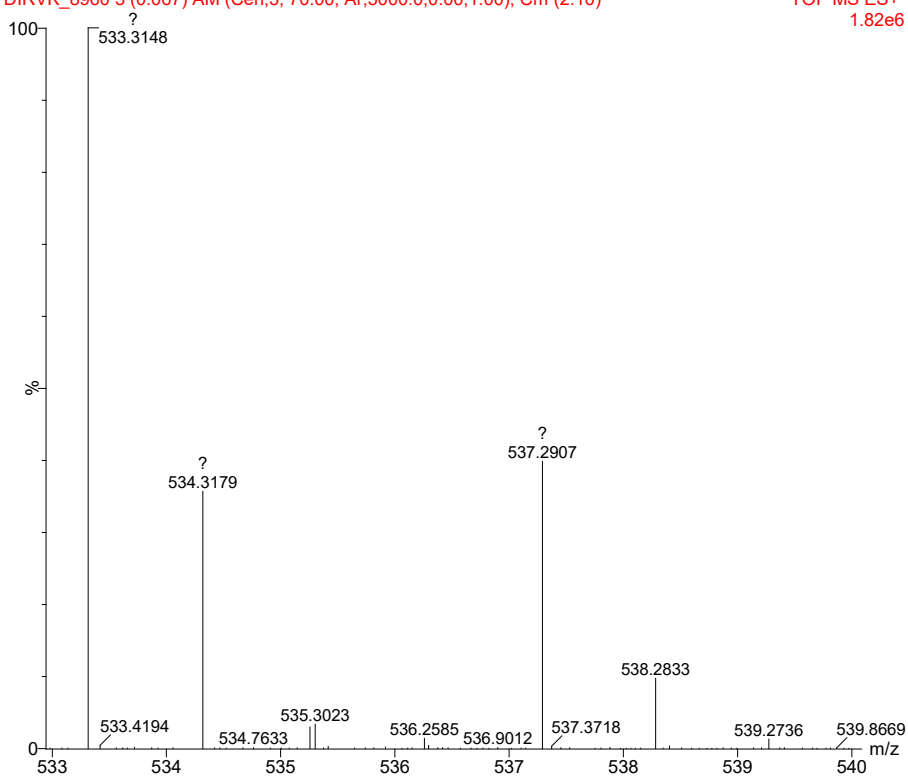


Mass spectra of compound 11h

direct infusion latky VK

DIRVK_8960 3 (0.067) AM (Cen,3, 70.00, Ar,5000.0,0.00,1.00); Cm (2:10)

TOF MS ES+
1.82e6

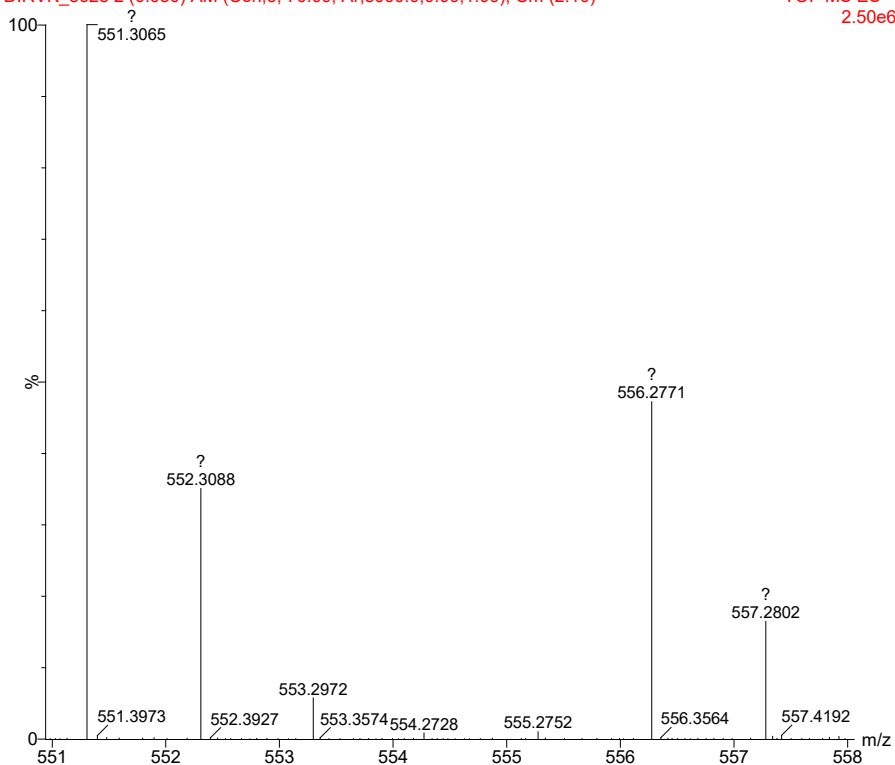


Mass spectra of compound **11i**

direct infusion latky VK

DIRVK_8628 2 (0.050) AM (Cen,3, 70.00, Ar,5000.0,0.00,1.00); Cm (2:10)

TOF MS ES+
2.50e6

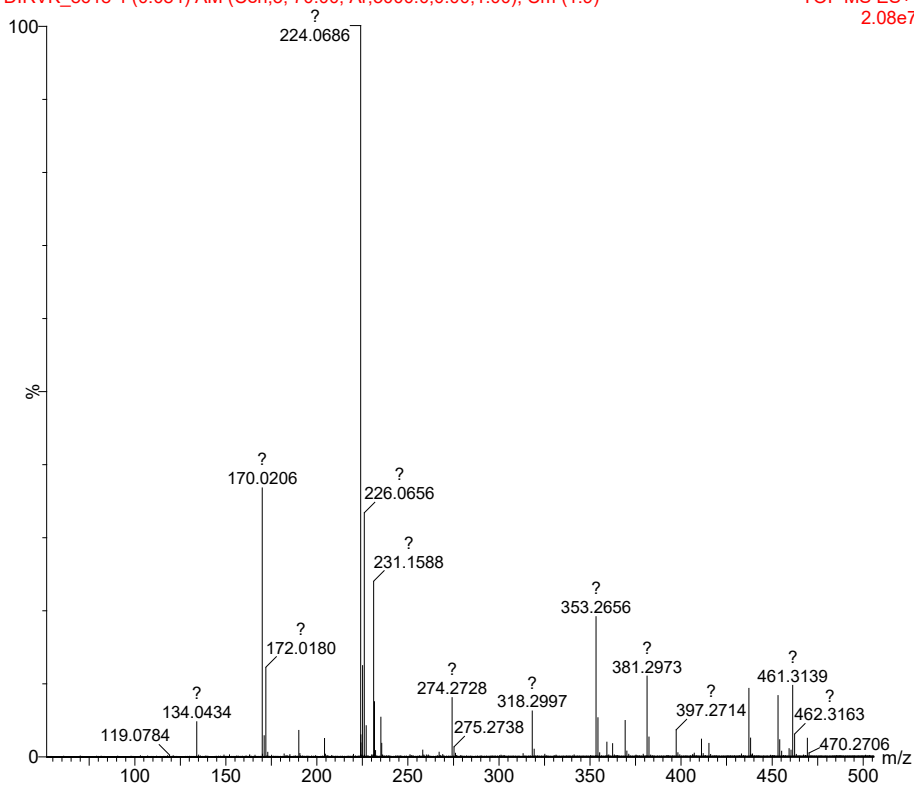


Mass spectra of compound **13a**

direct infusion latky VK

DIRVK_8618 4 (0.084) AM (Cen,3, 70.00, Ar,5000.0,0.00,1.00); Cm (1:9)

TOF MS ES+
2.08e7

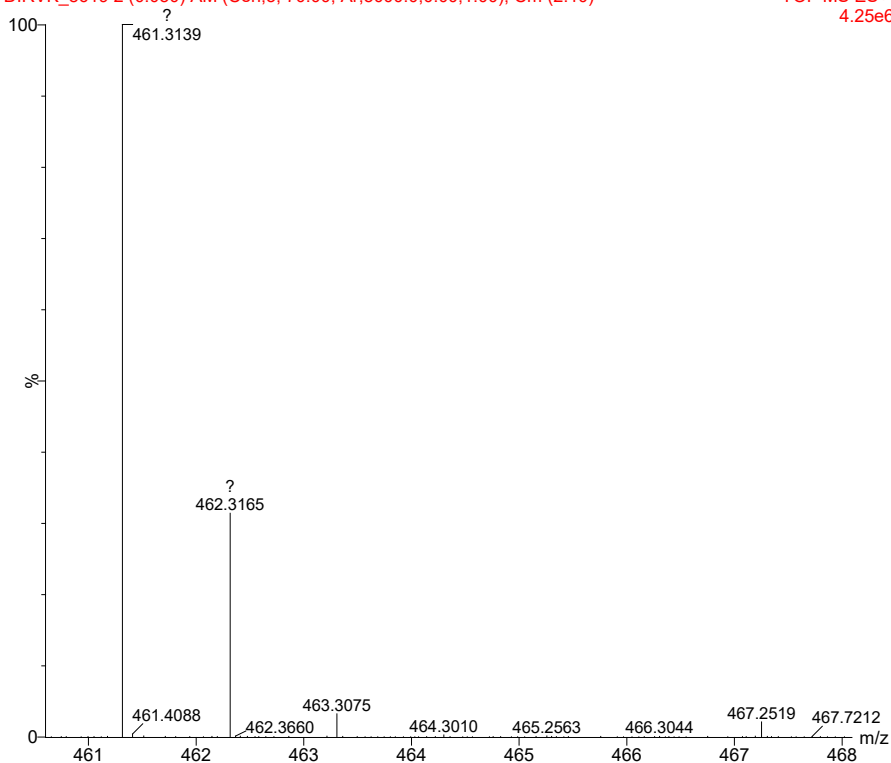


Mass spectra of compound **13b**

direct infusion latky VK

DIRVK_8619 2 (0.050) AM (Cen,3, 70.00, Ar,5000.0,0.00,1.00); Cm (2:10)

TOF MS ES+
4.25e6



Mass spectra of compound **13c**

direct infusion latky VK

DIRVK_8949 1 (0.034) AM (Cen,3, 70.00, Ar,5000.0,0.00,1.00); Cm (1:9)

TOF MS ES+
3.53e6

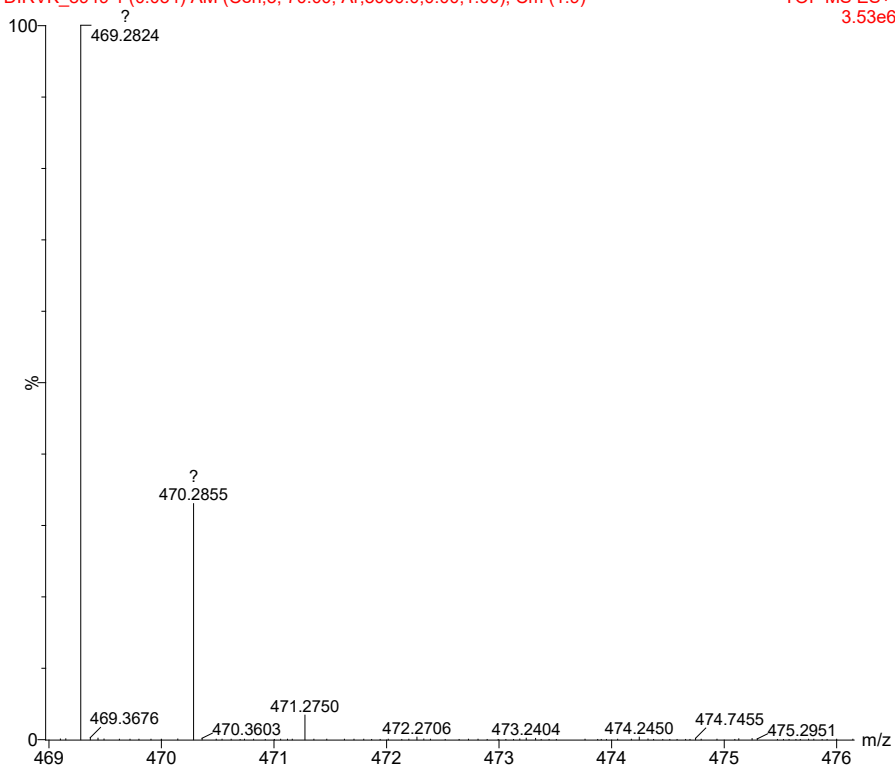


Table S1. Binding affinity scores (kcal/mol) of the purine derivatives with RDOCK, XP Score and MM-GBSA (ΔG_{bind} and their respective energy contributions) in the Bcr-Abl^{WT}.

Compd.	IC ₅₀	pIC ₅₀	RDOCK	XP Score	ΔG_{Bind}	$\Delta G_{\text{Coul.}}$	ΔG_{Hbond}	ΔG_{Lipo}	$\Delta G_{\text{Packing}}$	$\Delta G_{\text{Solv_GB}}$	ΔG_{vdW}
7b	0.220	6.658	-15.66	-8.51	-64.21	-15.29	-1.16	-22.94	-0.79	26.87	-56.66
7a	0.180	6.745	-14.38	-9.16	-59.92	-40.76	-1.37	-21.14	-1.48	51.6	-59.46
13c	0.840	6.076	-15.31	-7.74	-50.43	-15.57	-1.69	-19.3	-1.05	26.14	-51.97
13b	11.050	4.957	-14.22	-7.57	-51.13	-41.41	-1.76	-17.41	-1.07	47.1	-45.27
13a	3.950	5.403	-13.94	-7.51	-48.57	-8.79	-1.3	-16.44	-0.59	15.37	-47.62
11i	1.680	5.775	-15.15	-6.91	-55.34	-3.88	-2.29	-29.12	-0.66	19.24	-51.52
11h	0.670	6.174	-15.39	-7.33	-53.75	-10.36	-1.54	-20.23	-0.75	20.36	-50.32
11g	0.830	6.081	-13.19	-7.25	-52.36	-9.56	-1.47	-19.50	-0.70	20.50	-49.50
11f	1.760	5.754	-17.66	-8.57	-66.75	-18.34	-2.44	-24.09	-1.59	31.97	-53.41
11e	0.130	6.886	-17.33	-8.40	-65.32	-17.65	-2.30	-23.31	-1.47	30.23	-52.14
11d	1.240	5.907	-16.84	-8.20	-60.11	-16.48	-2.01	-22.32	-1.40	28.06	-51.04
11c	0.019	7.721	-19.04	-9.11	-74.32	-23.49	-2.7	-20.95	-0.89	24.31	-54.69
11b	0.014	7.854	-20.69	-9.36	-73.34	-24.39	-2.69	-20.92	-0.89	26.22	-54.71
11a	0.037	7.432	-17.49	-9.23	-71.06	-26.33	-3.07	-21.6	-1.16	29.25	-57.85
I	0.090	7.046	-15.19	-8.54	-57.16	-43.55	-1.24	-20.24	-1.23	48.37	-47.55
II	0.040	7.398	-16.91	-8.83	-60.04	-37.06	-0.83	-21.32	-1.53	45.94	-55.10
III	0.040	7.398	-16.54	-9.57	-59.74	-39.82	-1.19	-20.50	-1.24	42.57	-49.56
Purvalanol*	—	—	-31.45	-9.60	-69.69	-18.25	-1.90	-18.51	-1.46	15.06	-46.15
Dasatinib**	0.00014	9.854	—	-13.91	-87.55	-36.72	-2.12	-25.85	0.92	43.96	-58.09

ΔG_{Bind} = Binding free energy

ΔG_{Coul} = Coulomb energy

ΔG_{Hbond} = Hydrogen bonding correction

ΔG_{Lipo} = Lipophilic energy

$\Delta G_{\text{Packing}}$ = Pi-pi packing correction

$\Delta G_{\text{Solv_GB}}$ = Generalized Born electrostatic solvation energy

ΔG_{vdW} = van der Waals energy

ΔG_{Bind} = Binding free energy

*Docking score calculated with RDOCK, PDB: 6BL8

**Docking score calculated with PDB 2GQG

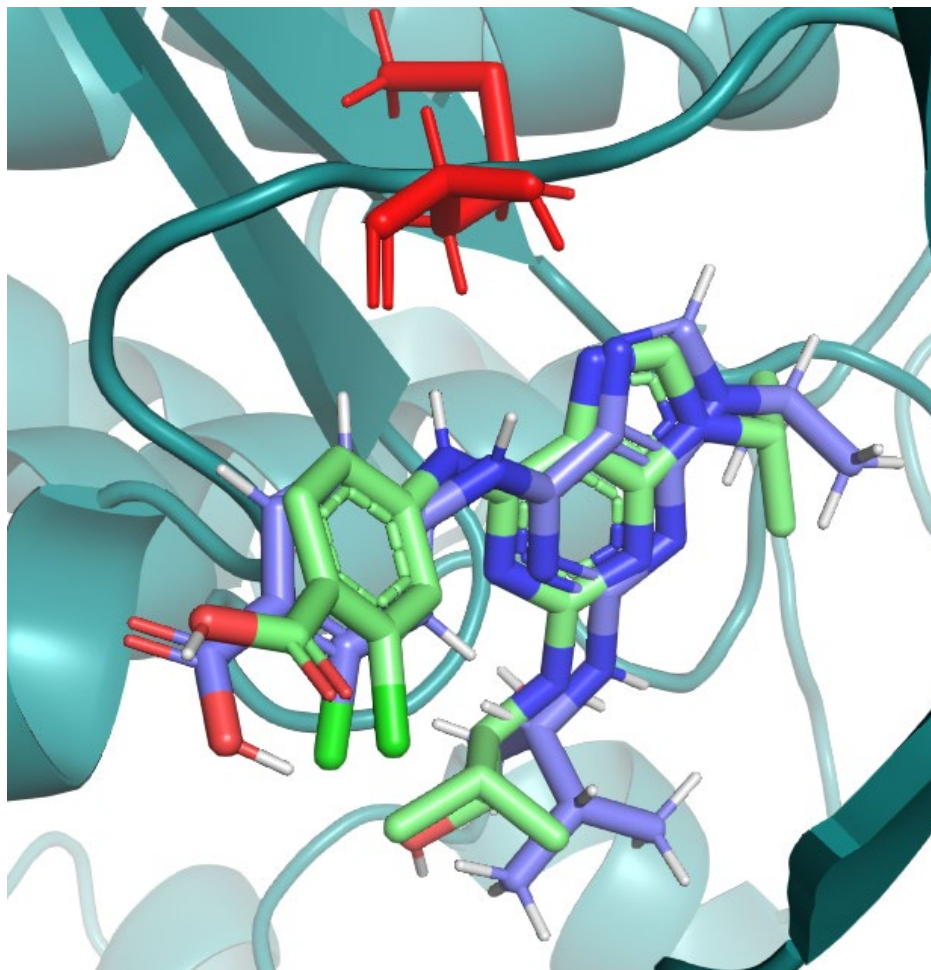


Figure S1. Co-crystallized ligand, purvalanol, in the Bcr-Abl binding site. Its experimentally determined binding mode is shown in blue, while the docking pose of purvalanol from our self-docking protocol is shown in green.

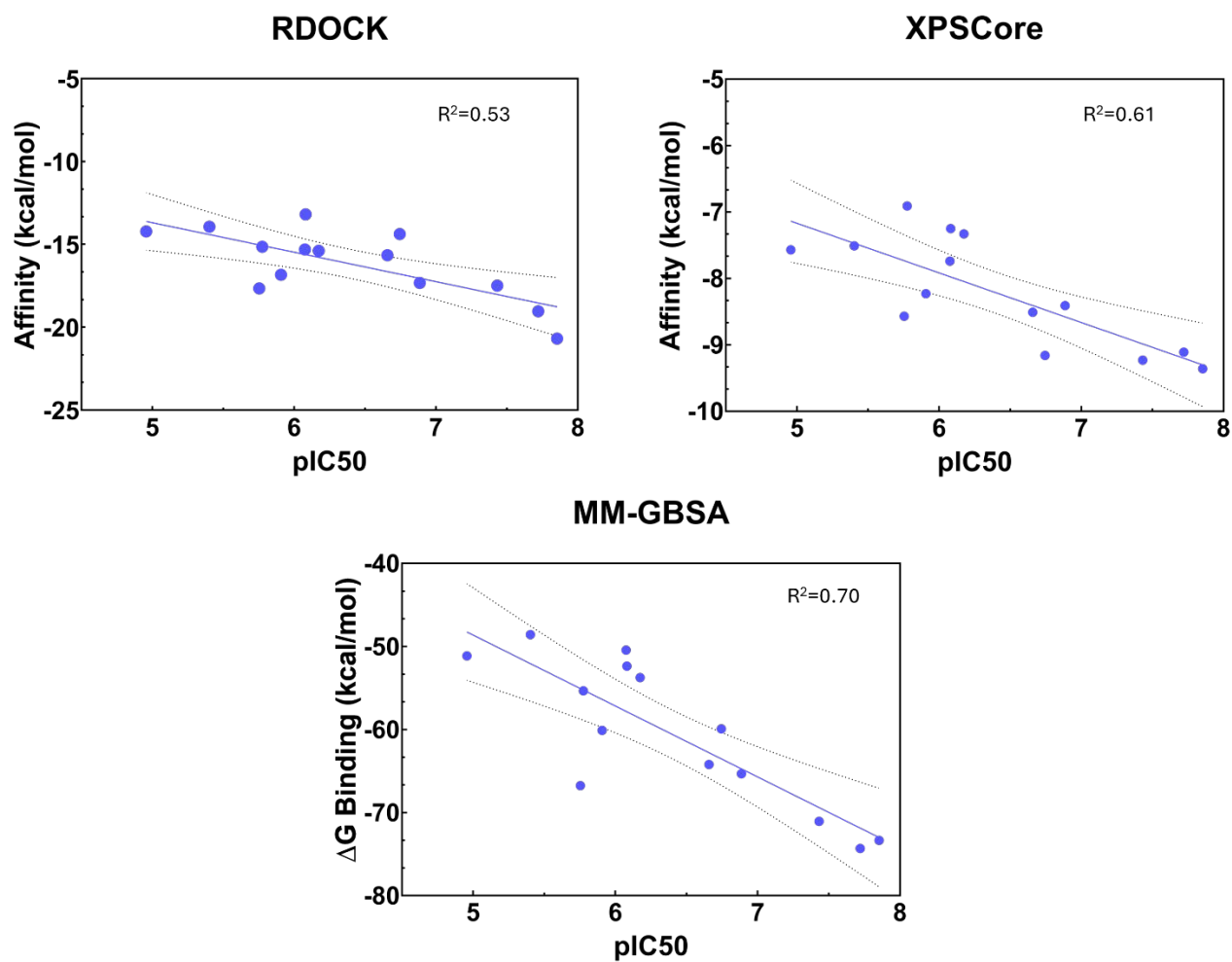


Figure S2. Correlation plot between biological activity in pIC₅₀ and affinity energies achieved with RDOCK, Glide (XP Score) and MM-GBSA of the synthesised compounds.

T315I (100%) KCL22B8 GI50			
Comp.	(uM)	SP Score	MM-GBSA
11c	9.06	-11.14	-65.17
11d	7.83	-11.48	-69.82
11e	6.91	-12.18	-71.67
11f	7.20	-12.12	-70.14

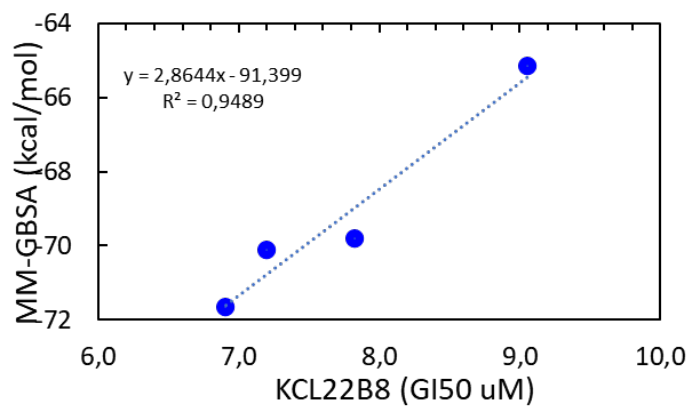


Figure S3. Correlation plot between biological activity in pGI₅₀ values on B8 cells and affinity energies achieved with MM-GBSA of the selected compounds.

Figure S4. Histograms of flow cytometry of selected compounds on KCL cells and their subclones.

